

Received January 22, 2020, accepted February 12, 2020, date of publication February 27, 2020, date of current version March 9, 2020.

Digital Object Identifier 10.1109/ACCESS.2020.2976526

# Ageing: Causes and Effects on the Reliability of Polypropylene Film Used for HVDC Capacitor

HAIDER M. UMRAN<sup>1,2</sup>, FEIPENG WANG<sup>1</sup>, (Member, IEEE), AND YUSHUANG HE<sup>1</sup>

<sup>1</sup>State Key Laboratory of Power Transmission Equipment and System Security and New Technology, School of Electrical Engineering, Chongqing University, Chongqing 400044, China

<sup>2</sup>Department of Electrical and Electronic Engineering, Faculty of Engineering, University of Kerbala, Karbala 1125, Iraq

Corresponding author: Feipeng Wang (fpwang@cqu.edu.cn)

This work was supported in part by the National Key Research and Development Program of China under Grant 2018YFB0905802, in part by the Chongqing Municipality under Grant cx2017041, and in part by the Project 111 of the Ministry of Education, China, under Grant B08036.

**ABSTRACT** It is well-known that the high-performance polymeric dielectric films used for high-voltage DC capacitors should have outstanding capabilities in terms of electrical and mechanical properties in order to face harsh operating conditions. Many factors limit the ability of these thin films to face different and growing stresses according to modern electrical requirements. Microstructure properties, additives, impurities, defects formed during manufacturing as well as applied stress types significantly affect the performance of dielectric films and their operational lifetime. This paper presents a comprehensive review of the factors which affect the ageing, degradation and breakdown of metallised polypropylene (PP) capacitors films. The effects of microstructure, surface morphological properties, mechanical properties and defects on the reliability of biaxially oriented polypropylene films (BOPP) are studied. In addition, the phenomena affecting dielectric performance and ageing mechanisms which are induced by electrical, thermal and electrothermal stresses are discussed.

**INDEX TERMS** Ageing, breakdown, crystallinity, deformation, electrical conductivity, microstructure, polypropylene, yield stress, reliability.

## I. INTRODUCTION

The increasing penetration of renewable energy systems and the urgent need for their reliable integration with power transmission systems that operate under diverse conditions have become major challenges. The functionalities of power quality can be improved by power electronics based-technologies, such as high voltage direct current (HVDC) converters, that apply capacitors as basic structural components. Therefore, the techniques and materials technology used to manufacture metallised polypropylene (MPP) capacitors have received considerable attention from researchers and manufacturers. MPP capacitors have been adopted given their numerous advantages, such as high voltages rates and low losses, self-healing and low cost, over foil-electrode capacitors [1]–[3]. HVDC capacitors are subject to various electrical and thermal stresses that affect their performance by different degrees in accordance with dielectric material quality and capacitor structure. The molecular structures,

The associate editor coordinating the review of this manuscript and approving it for publication was Cheng Qian.

conformations and orientations of polymers are important parameters that exert major effects on the macroscopic properties of the dielectric film used in capacitor applications [4], [5]. The adoption of biaxially oriented polypropylene (BOPP) films as state-of-art dielectric materials is one of the most important factors that distinguish the performance of MPP capacitors. Although BOPP films are linear dielectrics with excellent electrical properties, including low dissipation factor ( $\tan\delta \sim 10^{-4}$ ), high breakdown strength of up to 700 V/ $\mu\text{m}$ , low absorption and wide temperature range of up to 100°C, their energy density is low due to low permittivity (2.22–2.25) [6], [7]. Despite their ability to self-heal and their classification as a highly reliable component, MPP capacitors are subject to high stresses that lead to their failure [8]. Repetitive self-healing promotes metal evaporation, which consequently increases the internal pressure of the casing and enhances the rate of degradation [9]. Furthermore, partial discharge (PD) intensification results in electrical stresses that predispose adjacent regions to further electric breakdown because of the accumulation of vaporized metals and the increment in density its density to become conductive.

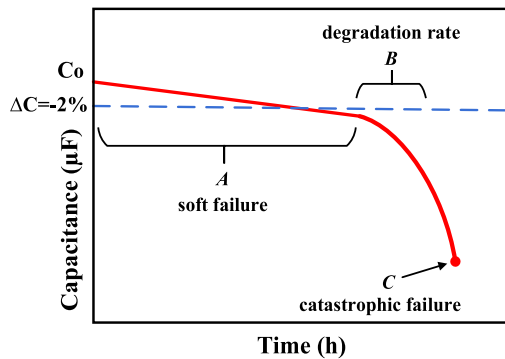


**FIGURE 1.** Typical capacitance decay of MPPC during degradation over time down to catastrophic failure (replotted from [10]).

These phenomena turn breakdown areas into conductive areas that induce flashover and catastrophic failure or burn the capacitor [9]–[11]. The long-term interaction of the electric field and heat under high voltages or harmonic current is the main reason for dielectric and electrode ageing [12]. The reduction in capacitance caused by self-healing (or clearing) is termed ‘soft failure’, wherein the capacitance value varies in accordance with manufacturers [13]. The capacitance degradation exhibited by MPPC over time is illustrated in Fig.1. Where A is the soft failure whose value is determined by the manufacturers and according to the application,  $\Delta C = 2\%$  in this case and B is the gradual increase in the degradation rate after soft failure until conductive vapor accumulated inside the capacitor leads to catastrophic failure at C. It worth mentioning that the degradation rate B depends on many factors like the presence of microvoids and /or defects in the dielectric, chemistry of polymer, somewhat less on molecular weight, thermal conductivity, and value of applied electric stress. The catastrophic failure C is represented as the breached or burning of the capacitor packaging and it may be caused by a build-up of pressure or flashover which leads to internal heating of the capacitor [10].

Unfavorable operating conditions, such as high voltage, current, frequency and temperatures and geometry effects, have remarkable effects on the deterioration, ageing and failures of capacitors [8], [14], [15]. Thus, the precise definitions of ageing, deterioration, breakdown and their interrelations are essential when considering the long-term reliability of a dielectric polymer. The processes that occur in the polymeric material over a specified period usually result in changes in the physical and chemical structure and the values of the characteristics of the used material. These changes are known as ageing. Degradation is a chemical change in the polymeric material that leads to undesirable changes in its characteristic values. Breakdown strength decreases as degradation progresses. Consequently, breakdown is defined by the abrupt and local loss of dielectric properties [16]–[18]. The ageing levels of capacitors can be classified in terms of electrical, thermal, electrothermal, chemical and physical ageing, as well as ageing arising from the specific geometry of the capacitor [10]. The final reliability of a capacitor is dependent

on the reliability, quality, suitability and safety of each of its components [14]. Understanding the causes, mechanisms and factors that accelerate the degradation, ageing and failure of capacitor components is necessary to enhance capacitor reliability.

This paper reviews the microstructure, morphology, mechanical and electric properties of dielectric films and the influence of defects, ageing types and other factors affecting its lifetime based on previous studies and related results.

The paper is organised as follows: Section II provides an explanation of the microstructure, morphological and mechanical properties and chemical defects of films. Section III discusses the thermal and electrical impacts on dielectric films. Section IV presents a survey of the behaviour of space charge and PD under different types of voltages and their relationship with the performance of dielectric films. The breakdown mechanisms of PP film are provided in Section V. Whilst Section VI presents the conclusion.

## II. FILM MICROSTRUCTURE AND MECHANICAL PROPERTIES

### A. STRUCTURE AND MORPHOLOGY

The excellent properties of BOPP films are attributed to molecular chains without polar groups that are oriented under the influence of the electric field [19]. Hence, their dielectric loss is essentially extremely low, and any potential increase in their dielectric loss is mainly due to the effect of residual catalysts, impurities and antioxidants. The linear increase in electrical conductivity and hopping conduction under the effect of strong electric fields and high temperatures are likely controlled by impurities. Thus, the crystallinity of BOPP films plays an important role in mitigating these phenomena [20]. The structural and morphological development of films during manufacturing can be considered as the main determinant of the final properties of the films [21]. In particular, a high-quality film includes the high isotactic (97 to 99%), 30 ppm (or less in ash content) with an optimum molecular weight distribution, minimum thermal shrinkage (or high thermal stability), homogenous thickness, controlled surface roughness, tensile strength and tearing resistance and smallest amount of residual catalyst content in the raw material [20], [22].

The factors that affect the dielectric breakdown strength of the film can be classified into essential factors related to compositional and morphological features (material) and procedural factors (nonmaterial) related to the active measurement area, electrodes, shape and voltage type, roughness and surrounding conditions [20], [23].

The structure and morphology of the film can be described on a hierarchical basis starting from the molecular chain, to the crystal structure, to the lamellar morphology, to the spherulitic morphology and finally to the microstructure [24]. Biaxially oriented isotactic polypropylene (BO-iPP) film can crystallise on the crystal structure level in three different forms (i.e. monoclinic  $\alpha$ , hexagonal  $\beta$  and orthorhombic  $\gamma$ ) depending on temperature, mechanical strain and

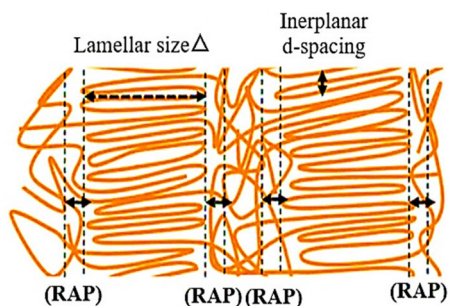


**FIGURE 2.** Semicrystalline structure showing the lamellar size  $\Delta$ , interplanar d-spacing and Rigid Amorphous Phase (RAP) [21].

pressure [21], [25]. The  $\alpha$ -form can be the dominant structure in the material, the  $\beta$ -form includes crystals that form under shear and the  $\gamma$ -form involves crystals that form under high pressure only [21], [26]. The BO-iPP film includes a crystalline phase that is characterised by high stresses, a mobile amorphous phase with a high free volume and low stresses and a hard amorphous phase that guarantees a chaotic transition between a highly ordered crystalline phase and a mobile amorphous phase [27].

The size of the crystalline and amorphous areas in these types of polymers is 10 nm, whereas that of the interfacial zone is 1 nm and has an important contribution to macroscopic characteristics.

The results of the Wide Angle X-ray Diffraction (WAXD) of three films with thicknesses 3.8, 7.8, and 11.8  $\mu\text{m}$  revealed that the 11.8  $\mu\text{m}$  film has the lamellar size  $\Delta$  (17.1, 15.2, 15.6, 14 and 24.2 nm) with reflection peaks (110), (301), (040), (130), and (400), respectively. While the orientation peaks of (400) and (130) for the 7.8 and 3.8  $\mu\text{m}$  films were absent. Calculations of diffraction peak (040) confirmed that the increase in the lamellae size  $\Delta$ ; 11.9, 12.9, and 15.2 nm corresponded with the increase in film thicknesses 3.8, 7.8, and 11.8  $\mu\text{m}$ , respectively. It should be noted that the crystallinity ratio and the lamellas size increase with the film thickness, consequently, the rigid amorphous phase increases as compared to the mobile amorphous phase associated with  $\alpha$ -relaxation [21].

The semicrystalline structure and three phases of BO-iPP film is shown in Fig.2

Micropore formation during the biaxial stretching of  $\beta$ -iPP films with thicknesses of 0.5 mm participates in the rotation and separation of  $\beta$ -lamellae and create cavitation in the amorphous phase between  $\beta$ -lamellae, whereas small lamellae are sheared. The bundle-like  $\beta$ -lamella, which is an incompletely developed spherulite, is an asymmetrical 3D structure with different tensile axis angles that cause various types of deformation during stretching [28]. Additional stretching beyond the yield point induces the development of the initial cavities into large pores, the transformation of the  $\beta$  phase to the  $\alpha$  crystal phase and the stress-induced break-up of lamellae [29]. iPP films with mixed  $\alpha/\beta$ -phases may also suffer from the same mechanisms that underlie void and porosity formation on the surface [20].

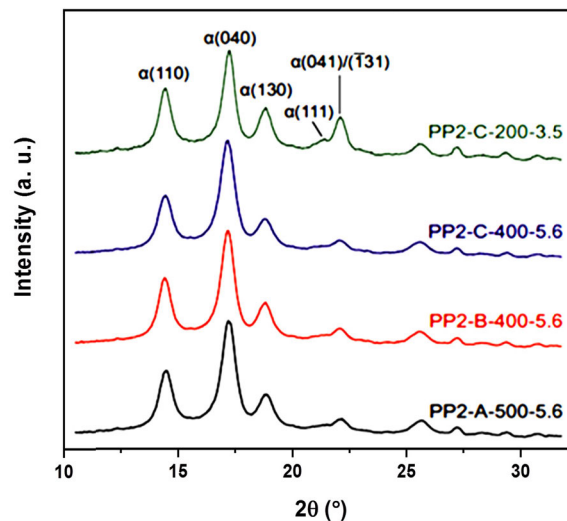


**FIGURE 3.** WAXRD profile of BOPP films (replotted from [20]).

The effect of the crystalline and polymorphic structures of BOPP films with varying thicknesses and subjected to different treatment methods have been tested. Cast film samples and biaxially stretched films were coded as PP1 homopolymers and PP2 high isotacticity grade. A, B and C have indicated the extrusion types and 500, 400, 200, 15 and 20 determine the cast film thicknesses, while 5.6 and 3.5 were represented the stretch ratio.

It should be noted that the types of extruder used were as follows: extruder A is a small-scale mono screw extrusion machine consists of flat mold, melt pump and a screen pack with three-layer filters set, it operates at a high screw compression ratio (4:1) with extrusion pressure 80 bar for 500  $\mu\text{m}$  cast film. Extruder B is a large-scale mono screw extrusion machine formed of a screen pack with a filter. Operating at the screw compression ratio (1.5:1), it adopted to produce the 400  $\mu\text{m}$  cast film. While extruder C is a small-scale mono screw extrusion machine consists of dense filters. Operating with a low screw compression rate (1.5:1), it was used to produce both thick (200 and 400  $\mu\text{m}$ ) and thin (15 and 20  $\mu\text{m}$ ) cast films.

As illustrated in Fig.3, the Wide-angle X-ray Diffraction (WAXRD) crystalline structure test revealed that  $\beta$ -form crystallinity is almost completely absent because of extensive strain-induced crystal transformation (from  $\beta$  to  $\alpha$ -form) [20].  $\beta$  to  $\alpha$  transformation starts during the pre-heating phase at 125 -140°C from the desired heating period that precedes the axial expansion of the film [30]. The film subjected to biaxial stretching is naturally weak in the (110) plane orientation.

The stretching of the residual  $\beta$ -phase throughout the first stage of orientation is responsible for cavitation on the film surface [20]. The diffraction intensity peaks indicate that the crystallinity increases with the thickness and ratio of biaxial stretching.

The smaller crystal size usually leads to higher breakdown strength of films with intermediate forms between

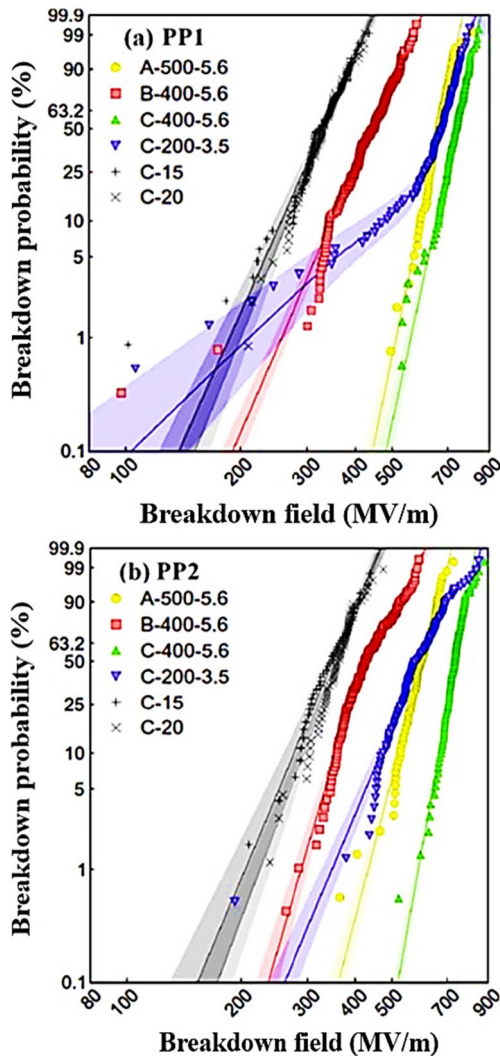


FIGURE 4. Large-area DC multi-breakdown distributions of, (a) PP1- and (b) PP2 of BOPP films and thin cast films (replotted from [20]).

nonoriented spherulitic–lamellar and highly oriented fibrillar morphologies, such as C-200-3.5 film. Although iPP grades determines the breakdown strength because the content of the  $\beta$ -phase is inversely proportional to film breakdown performance, the biaxial stretch ratio also plays a significant role. The non-oriented cast films exhibited comparable breakdown characteristics with the biaxially stretched films at initial breakdown fields in the range of  $\sim 360\text{--}400\text{ V}/\mu\text{m}$  (Fig.4).

The PP1-C-200-3.5 film indicated deflection and numerous breakdown mechanisms. While the cast films C-15 and C-20 not shown a significant dependence on thickness in the breakdown mechanism. A somewhat higher trend of  $\beta$ -crystal content for the cast film is reflected in the breakdown properties of the biaxially stretched PP2-A-500-5.6 and B-400-5.6 films. The increase in biaxial stretch ratio that reduces the sizes of crystallites perpendicular to the stretching plane accounts for the differences by the breakdown strength between C-200-3.5 and C-400-5.6. The differences between iPP grades reduce in accordance with the decrement in the relative  $\beta$ -phase content of the initial cast film (C-400-5.6) and

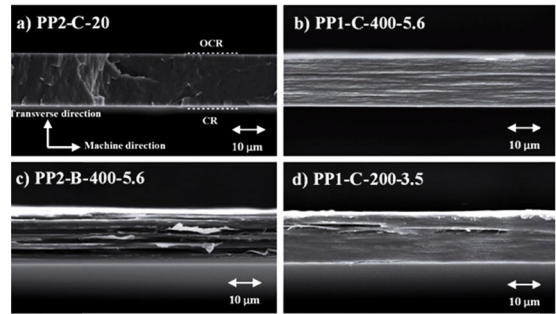


FIGURE 5. Cross-section SEM images of cast and BOPP film samples (replotted from [20]).

result in excellent dielectric strengths of  $\sim 750\text{ V}/\mu\text{m}$  [20]. The degree of BOPP film crystallinity slightly increases as the equibiaxial stretch ratio increases [31], and the electrothermal breakdown strength of the field-dependent electrical conductivity decreases [32]; as such, the amount of trapped charges at the boundaries of the amorphous crystalline structures increases [33]. The change in molecular structure to a crystal-like structure may enhance thermal conductivity by reducing phonon scattering [34]. The crosslinking of the polypropylene (PP) film increases mechanical strength and thermal stability and consequently increases dielectric strength; thus, network stability remarkably decreases the chain mobility that is required to form a free volume or defects under strong electric fields [35].

Film roughness is another factor that affects breakdown strength. Surface roughness at the interface of electrode-dielectric may strengthen the local electric field near surface and thus intensifies charge carrier injection and space charge accumulation in the material [36]. These unfavourable effects affect breakdown behaviour [37]. In the context of film morphology as well, it was found that the melting-peak shifts to a somewhat higher temperature with an increase in the stretching ratio and drawing temperature, while the width of peak slightly narrows. The slight decrease in peak width refers to the structural transformation from lamellar to oriented structure, i.e. transfer from the weakest (thermal stable) lamellae to the strongest one. On the other hand, thermal stability in the oriented structures can be attributed to the healing of defects that occur during stretching, which would improve the breakdown strength of BOPP films [38]. Anyway, the transformation of spherulitic cast film morphology to extremely oriented fibrillar morphology during a biaxial stretching of the film is key factors leading to a superior of BOPP breakdown strength [6].

The cross-sectional optical microscopy (OM) images of cast films revealed a spherulitic morphology of skin-core type what confirms the presence of  $\alpha/\beta$  spherulites mixture and a transit crystalline evolution (Fig.5, a and b) [20].

The cast film image (PP2-C-20) revealed a granular surface structure for both chill roll (CR) and the opposite side of the chill roll (OCR). The increase in the mean surface roughness was proportional to film thickness. The cast

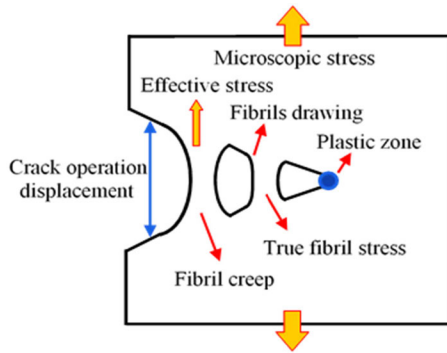


FIGURE 6. Craze-crack and craze propagation (replotted from [136]).

film's initial spherulitic morphology properties are deformed through biaxial stretching process, to the highly-oriented fibrillar structure. On the other hand, the OM images of the BOPP films showed big variations in film transparency, depending on cast film initial  $\beta$ -crystallinity.

Besides, existence of various amounts of porosity and voids parallel to film surface was observed [39], [40]; which were mainly correlated with  $\beta$ -form crystal index ( $k_\beta$ ) of the cast film (Fig. 5, c and d).

### B. MECHANICAL PROPERTIES

Polymer films exhibit elastic properties that vary widely in accordance with their microstructure and processing conditions [41]. Thus, understanding the quantitative relationship between crystalline structure and elastic modulus is important to determine the mechanical properties of films required for specific applications [42]. Shear yielding and crazing are two important polymer deformation micromechanisms that represent the main source of material energy absorption. The difference between these mechanisms is that shear yielding occurs when the volume is constant, whereas crazing occurs as volume increases; hence, crazing is a cavitation process [43].

Crazes form when the external tensile stress causes microvoids to nucleate at points of high-stress concentrations generated by surface scratches, defects, cracks, dust microparticles and heterogeneity in the polymer [44]. Microvoids are formed at the gaps between broken particles on the shear bands. Microvoid formation on the external surface is considered as cracking initiation [45]. Microvoids propagate on a plane perpendicular to the highest maximum stress and stabilise temporarily within fibrils that span the craze. Thus, the crazed crack transition is the beginning of the actual failure mechanism [43], [46].

A schematic of the craze stress mechanism is provided in Fig.6.

Shearing is more effective as a plastic deformation mechanism than crazing in terms of energy dissipation because the whole volume of plastic-deformed material is shared in energy dissipation. Crazing is linked to brittle failure, whereas shearing is linked to ductile failure; hence, these transitions are referred to as brittle (B)/ductile (D) transitions.

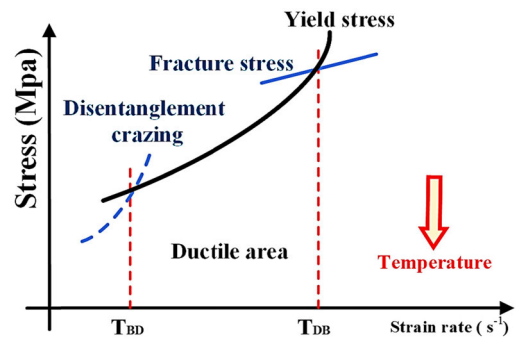


FIGURE 7. Strain rate Davidenkov plot for DB and BD transitions at low and high strain rates (replotted from [137]).

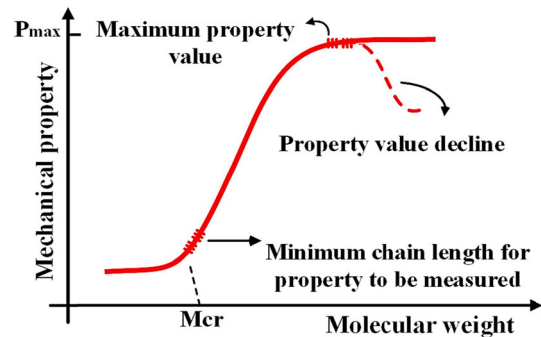


FIGURE 8. Polymer mechanical properties as a function of molecular weight (replotted from [48]).

A highly deformed fracture area represents a ductile fracture mechanism, whilst the least locally distorted area indicates a brittle fracture [47].

Semicrystalline polymers experience two BD and DB transitions ( $T_{BD}$  and  $T_{DB}$ ) and a shear plateau between these transitions. Fig. shows the ductile plateau as a function of strain rate.

The mechanical properties of linear polymers, such as PP, depend on molecular weight. Linear polymers exhibit favourable strength at a critical molecular weight. Polymer mechanical properties increase beyond a critical molecular weight to a second critical molecular weight. The dependence of mechanical properties on average molecular weights decreases or disappears at this second critical value, as illustrated in Fig.8.

Nonpolar polymers are characterised by an appropriate range of molecular weights between critical values, whereas polar polymers and polymers containing hydrogen exhibit optimal mechanical properties at low molecular weights [48], [49]. The dielectric films used in capacitors, however, must have sufficient tensile strength to withstand the pressure applied on the film layer when they are rolled tightly to prevent air gap formation. The tensile strength of most films is between 160–200 MPa and depends on film microstructure [50].

The simulation results for the crystalline structure effect test of isotactic PP films on elastic modulus indicate that enhancing chain regularity increases modulus by increasing

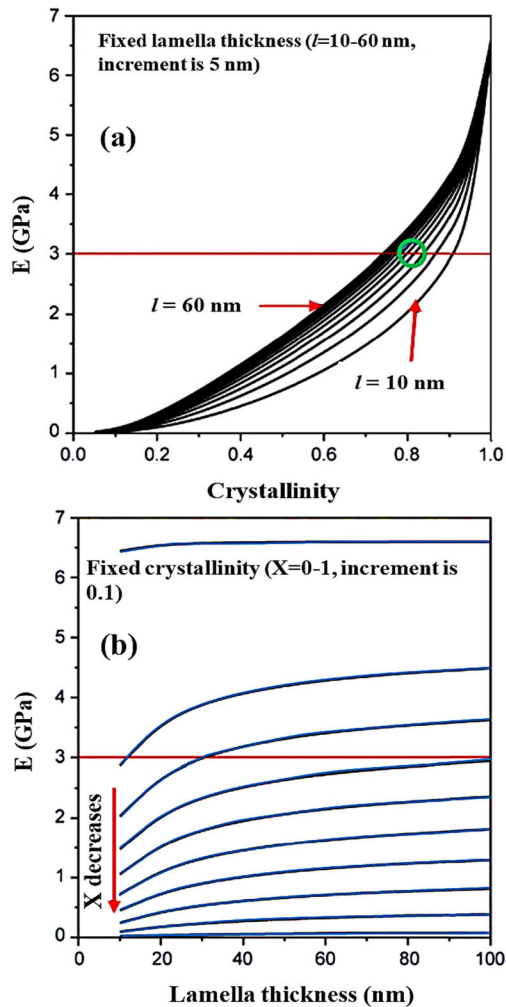


**FIGURE 9.** Prediction of modulus values based on, (a) fixed lamella thickness and (b) fixed crystallinity values (replotted from [42]).

crystallinity and lamellar thickness. Lamellar thickness has a weak effect on stiffness, and a thick lamella increases modulus at the same crystallinity level, as shown in Fig.9a; the improvement in crystallinity is illustrated in Fig.9b [42].

Thus, microstructure and orientation degree have a remarkable effect on electrical and mechanical properties and the general behaviour of dielectric films subjected to electrothermal activation and temperature, strain rate, stress state and shape and size defects. Thermal ageing stimulates chemical reactions in polymers that lead to chain scission and reduce molecular length and weight [51]. Consequently, the reduction in molecular weight as a result of chain scission reduces mechanical strength and leads to the low ductility of the material [52]–[54]. The presence and propagation of microvoids in dielectric films under the influences of stress initiates PD ageing and breakdown mechanisms.

### C. CHEMICAL DEFECTS

Potential chemical defects in a polymer structure are one of the important causes of film function degradation during application. Functional density calculations indicate that

impurities in the band-gap result from chemical impurities in PP [55], [56] and lead to electron density interference between polymer backbones. As such, charge carriers hop between valence and conduction bands, the conductivity of the material is increased and thermal breakdown is facilitated [57]. Although PP has an impressive band-gap of 7eV, the effect of its defects and impurities that contained cannot be ignored. The electronic band-gap value is a good index of polymeric dielectric quality and is highly correlated with breakdown strength [58].

There are six possible chemical defects in the electronic structure of the polymer chain. When a single hydrogen atom is removed from each of two adjacent carbon atoms, the double bond defect forms ( $-\text{CH}_2\text{CH}_2-$ ). The defect of hydroxyl (OH) is formed when a hydrogen atom is replaced in a C–H bond by  $-\text{OH}$  group. Whereas, the carbonyl ( $\text{C}=\text{O}$ ) and vinyl defects are formed when the two C–H bonds of a carbon atom are replaced by an oxygen atom and a  $=\text{CH}_2$  group, respectively. On the other hand, the conjugated double bonds ( $-\text{CH}_2=\text{CH}-\text{CH}=\text{CH}_2-$ ) are created when one C–C bond occurs between two double bond defects. Accordingly, dienone ( $-\text{CH}=\text{CH}-\text{CH}=\text{O}-$ ) is the combination of a double bond and a carbonyl defect.

Distinct occupied and unoccupied levels in the band-gap exist in the case of C = O, vinyl, conjugated double bond and dienone defects while are separated by a 5 - 6 eV. These defects are partly responsible for the reduction of breakdown strength by decreasing the band-gap of a dielectric [59].

## III. THERMAL AND ELECTRICAL IMPACTS ON DIELECTRIC FILMS

### A. THERMAL IMPACT ON FILM

The charging/discharging cycles generated from electrodes and dielectric materials cause thermal ageing by increasing the internal heat and energy losses of the capacitor [10], [60]. The numerous factors that cause thermal ageing are discussed in this paper. Thermal ageing is one of the most important factors that results in the serious degradation of dielectric material properties and the failure of capacitors.

A perfectly pure polymer film (where all of the films are contaminated by ambient air or grease stains or are contaminated deliberately or during manufacturing) does not exist [61]. No polymer film has a fully crystalline grade, that is, polymer films exhibit varying degrees of crystallisation; for example, BOPP films include crystalline and amorphous zones [62], [63]. The dielectric loss of the BOPP film is 0.0002 at temperatures up to 85°C and considerably increases because of electronic conductivity as temperatures exceed 85°C [64], [65]. Excessive heat morphologically changes dielectric materials [62]. High film purity, antioxidant amount and impurities are critical factors that affect film performance at high temperatures and under strong electric fields. The PP polymer is susceptible to free radical-mediated chain degradation because each of its monomer units has a tertiary proton [66]–[68]. Antioxidants represent a catalytic mechanism that rapidly degrades polymer chains by removing

the labile tertiary hydrogen ( $H^*$ ). Thus, the resulting spontaneous oxygen oxidation of the polymeric carbon radical is followed by hydroperoxide group formation. After the hydroperoxide group is decomposed, two potential degradation mechanisms of the polymer chain create two pairs of PP chains with reduced molecular weight. Two new polymeric carbon radicals are created simultaneously with constitute PP polymers along with a terminal aldehyde or an unsaturated group [69], [70].

Thermal ageing rearranges part of the crystallinity phase via molecular packing and enhances the crystalline phase and the recrystallisation of the thermally unstable crystalline zone [4], [71]. The crystalline and amorphous regions in polymeric materials have a direct effect on the final physical properties and ageing of capacitors during application [71].

Thermal ageing results in the conversion of part of the amorphous phase of the film to the crystalline phase and an increase in the amounts of high molecular-weight materials in the surface layer, where impurities and low-molecular-weight materials have been rejected from the bulk materials in the aged film. Consequently, the amount of impurities and low molecular-weight materials on the surface layer of the film increases as the crystalline phase increases [4], [62], [72]. The amorphous region is affected by high temperatures given its low melting point. The high-temperature region causes ion hopping and activates the current conduction mechanism in the amorphous phase [4], [64]. Regardless of the remarkable crystallisation that occurs in aged films, the conduction current dramatically increases after thermal ageing. The conduction current mechanism is attributed to the relaxation of the oriented amorphous phase and/or an increase in ionic concentration [73]. Increments in temperature result in a chemical change in the polymer film and act as the thermal activator of chemical reactions that are inert at low temperatures [4], [62]. The thermal activation energy of the BOPP film is 0.76eV [64]. Supplying excess energy to the macromolecule chains may cause polymer degradation and eventual breakdown due to that energy concentrated on chemical bonds significantly elevate energy levels beyond activation energy [15]. These chemical reactions are followed by the free-radical formation, wherein the presence of a free radical or a single electron increases molecular instability [74]. This condition ensures that additional chemical reactions with the surrounding compounds are initiated, oxygen is absorbed (oxidation), moisture is generated (hydrolysis), compounds are depolymerised (i.e. reactions between different polymer chains) or the backbone chain is divided or crosslinked. Fig.10 shows the polymer network that is induced by stress at temperatures above the glass transition temperature [15], [75].

The results of the thermogravimetric analysis (TG) have revealed that the more aged samples are rapidly degraded. The temperatures of the aged samples under the natural solar environment decreased for 60 and 80days from 443 to 439 °C, respectively compared to the reference sample 452°C (Fig.11).

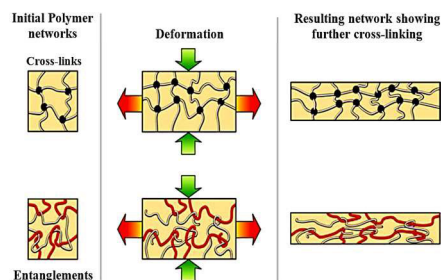


FIGURE 10. Polymer networks stress-induced at temperatures above  $T_g$  (replotted from [138]).

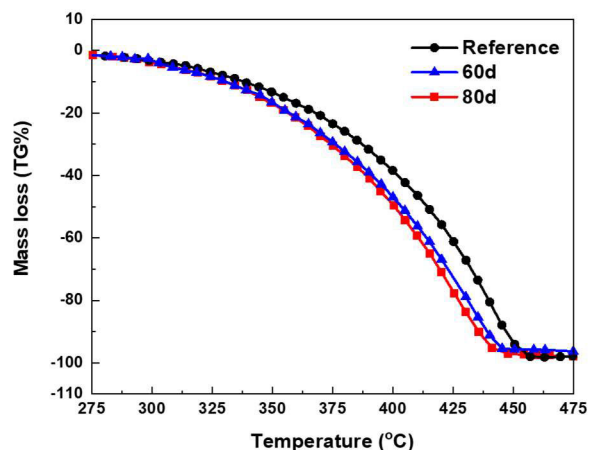
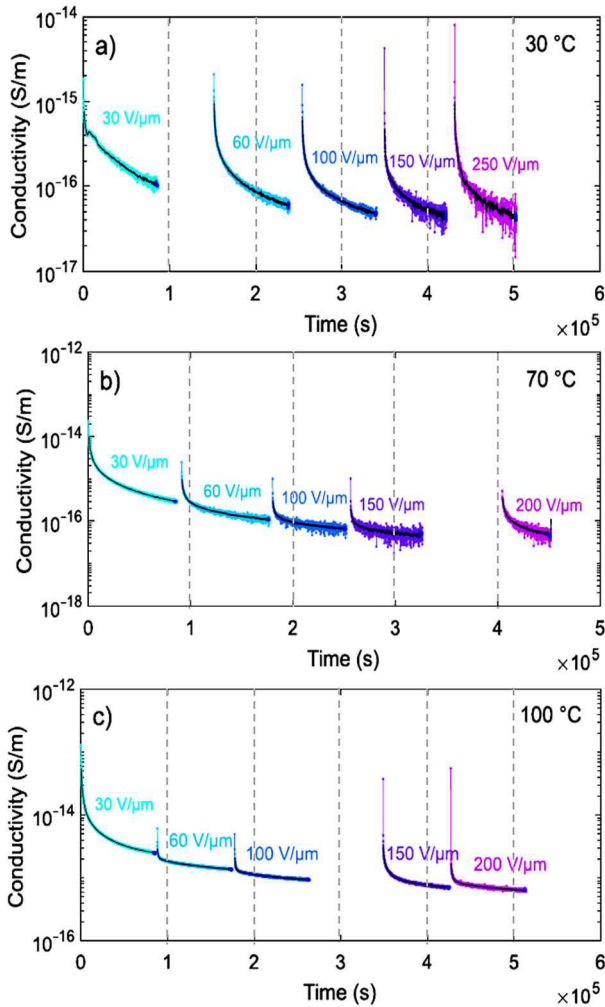


FIGURE 11. TG curves of the PP samples. (replotted from [76]).

For the same temperature, the percentage of the corresponding mass loss increased as a function of the ageing period [76]. Segments of the degraded polymer by thermal ageing leads to displaced the initial temperature of the sample to lower value. The higher difference in temperatures between aged and reference samples may be attributed to the chain scission effect [77].

Conduction is another source of loss in capacitor films and is coupled with the hopping mechanism when the charged carriers (electrons) hop between traps. The hot electron jump distance was approximately 1.4nm at 308K for a BOPP film with 7  $\mu\text{m}$  thickness [64], [78]. Carrier mobility is activated thermally under a weak electrical field ( $<10$  MV/m) when the energy gained between traps is lower than thermal energy and conductivity is Ohmic. The energy gained from a strong electric field ( $\geq 100$  MV/m) when a carrier moves between traps becomes comparable with thermal energy; this effect initiates detrapping that leads to an exponential increase in conductivity under an electric field [64]. The transition from Ohmic to nonlinear conduction for BOPP films occurs at 100MV/m. Thus, under sufficient electric field strength, the energy gained between traps approaches the depth of the trap to activate trapped carriers; however, ageing rapidly evolves and the dielectric polymer enters the prebreakdown stage [64], [79].

The effect of temperature on the DC conductivity behavior of BOPP films with Ni/Au electrodes at different



**FIGURE 12.** Conductivity of 10  $\mu\text{m}$  BOPP versus time with the gradual increment in DC voltage and different temperatures (replotted from [80]).

temperatures (30, 70, and 100°C) under 30–250 V/ $\mu\text{m}$  electrical fields has been reported. Conductivity remarkably increases as the temperature is increased from 30 to 100°C but also gradually decreases and becomes slowly saturated over time; however, a clear dependence on the size of the electric field over the range of 30–250 V/ $\mu\text{m}$  is absent [80], as in Fig. 12.

The measured properties cannot be directly linked to BOPP only because evaporation may alter the physical, chemical and electrical properties of the metal BOPP interface [81], and gradual morphological changes have potential effects during measurement (e.g. secondary crystallisation at increasing temperatures). The electrical conductivity of BOPP depends on the hopping mechanism. The hopping distance ( $\lambda$ ) ranged from 1.4nm to 3.2nm when temperature increased from 308K and 373K, respectively, with activation energy approximately 0.75eV independent of the electric field [64]. The density of conduction current as a function of the electrical field at different temperatures is illustrated in Fig.13.

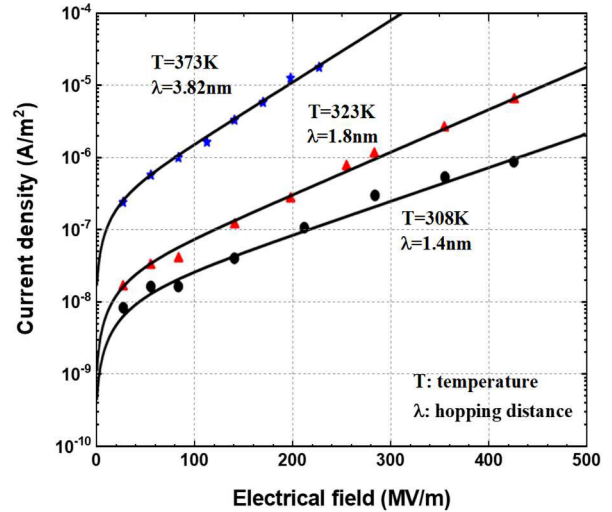


**FIGURE 13.** Conduction current density of the 7  $\mu\text{m}$  BOPP film as a function of electric field strength at different temperatures (replotted from [64]).

Nonetheless, the distance value of hopping ranged depend on the dielectric film crystallization’s degree [6], [64]. While high temperature activates additional carriers to contribute in conduction at a very low electric field [82].

The conductance losses of the dielectric polymer increase as its conductivity increases under a strong electric field and at high temperature; thus, thermal ageing is a major impediment to the reliability of dielectric polymers [64], [83].

**B. ELECTRICAL EFFECTS ON FILM**

Polymer materials contain varying proportions of impurities, micropores, amorphous regions, straight chains, string folding, fibre tufts, chain ends, dislocated regions, residual catalysts and additives (polar groups) used by manufacturers [84]–[86]. These exotic materials and physical defects cannot maintain neutrality under the influence of a certain electric field strength but contribute to the formation of space charge traps [87]. The first stage most likely initiates the deterioration of the polymer film under the influence of electric field intensity during macromolecule ionisation due to electron tunnel transfer [88]. Direct degradation of dielectric film can be classified into two levels in accordance with electric stresses: the breakdown of low-density regions (PDs), which have an extremely aggressive interplay with the polymer surface, and the direct effect of electrons on the polymer layers near the electrode/dielectric interface (space charge) [89], [90].

The application of an electric field with a strength exceeding the threshold of the dielectric material results in polarisation that stems from trapped of the space charge, which consequently enhances the local electrical field and distorts the applied field distribution and leads to electrical ageing [91]–[93]. On the other hand, another study revealed that the origin of ageing is mainly by mechanical stress (shear, compression, and torsion) and that space charge is a result

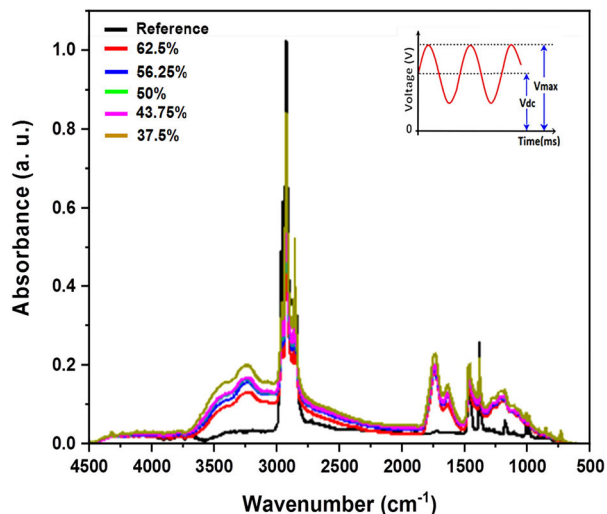


FIGURE 14. FTIR-ATR results for PP films (replotted from [92]).

of mechanical ageing. The accumulation of space charge in a degraded film by ageing strengthens the local field and leads to breakdown. Whereas initial degradation has already occurred due to electromechanical deformation in the molecular chains of polymer [63].

Electrostatic energy plays an important role in the configuration of a particular set of charges within the dielectric and thus increases with the electric field and ultimately becomes equal to polymer cohesion energy. Van der Waals attraction bonds are inevitably broken under an equal or higher value than that of the critical field. Given that the energy of PP cohesion is usually low ( $\sim 0.1\text{eV}$ ) the energy barrier is distorted by the energy of cohesion and results in irreversible ageing [63], [91]. The melting point of PP film is  $160^\circ\text{C}$  during accelerated ageing at a set temperature of  $110^\circ\text{C}$ .

A previous study carried out to the PP films were aged under different voltage stresses. DC% determined as a ratio of the variable DC-voltage to the combined (AC and DC) voltage which was represented as the maximum voltage ( $V_{\text{max}}$ ), ( $\text{DC}\% = (V_{\text{dc}}/V_{\text{max}}) \times 100\%$ ). The  $V_{\text{max}}$  was set as a fixed voltage at 5kV with 1kHz.

Identified values of (DC%) were 37.5%, 43.75%, 50%, 56.25% and 62.5%. The FTIR-ATR spectra and the combined voltage waveform are shown in Fig. 14.

The new peaks that emerged in the FTIR-ATR spectra of aged samples represent O-H and C = O groups. The intensities of these groups are higher than those of groups in virgin samples. Consequently, the growing number of new molecules enhances oxidation and increases the breaks in the long polymer chains; these effects promote film degradation [92]. PD is enhanced and chains are in scission when the AC voltage increases (or D% decreases). Thus, long chains are broken into small chains.

The occurrence of oxidation and the formation of polar molecules, such as -OH and C = O, intensifies orientation polarisation and increases the dielectric constant, as shown in Fig. 15 [92], [93]. Only DC stress may induce crosslinking

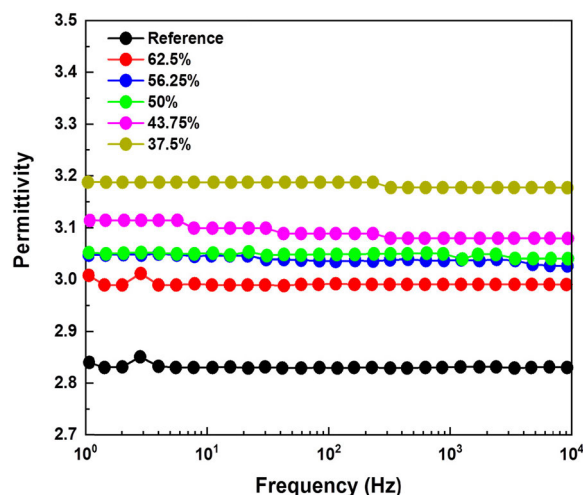


FIGURE 15. Permittivity of aged PP films (replotted from [92]).

by producing -OH groups and carbonyl groups; by contrast, AC stress may induce polymer degradation by producing numerous -OH and carbonyl groups via the frequency effect [93], [94].

#### IV. SPACE CHARGE AND SELF-HEALING UNDER VARIOUS VOLTAGE WAVEFORMS

##### A. SPACE CHARGE

Most polymer dielectric films utilised in capacitors are subjected to strong electrical fields, whether AC, DC or superimposed, that lead to space charge injection and accumulation in varying proportions in accordance with the applied field type [95]. Given that defects exist in polymer films, positive and negative charges be in an unequal state due to asymmetric atomic distribution in the defects, carriers will be attracted thus form charge traps [87], [89]. The space charge accumulation can lead to distortion of the local electric field in the dielectric [96]. This process generates electromechanical stresses that lead to the deformation of the molecular chains of the material, thus initially resulting in property deterioration and accelerating dielectric material ageing [63], [97]. The traps are classified as shallow and deep on the basis of activation energy [98]. Deep traps are formed in BOPP films when activation energy exceeds 1eV, whereas shallow traps are formed when activation energy is less than 1eV [89]. Polar groups, impurities, and catalysts are polarised under a low DC electric field to form a homocharge (symmetric polarity with the field) inside the dielectric. While the heterocharge (asymmetric polarity with the field) forms inside the film as a result of injecting the charge under a higher electric field. The formation of heterocharge would strengthen the electric field near the electrode and reduces it in the middle of dielectric, which may reduce the breakdown voltage, unlike the effect of homocharge [89], [99].

However, measurements of the space charge can provide useful information on charge density, investigate charge injection and transport mechanisms and behavior of the electric field in the dielectric, and thus in the ageing process [100].

The formation of space charges within the dielectric depends on the crystalline morphology of the semicrystalline polymers, film thickness, and physical defects such as micropores and cavities. These physical defects are formed by the local arrangement of molecular chains to act as carrier traps for the space charge. The behavior of space charges is totally different depending on the crystallinity degree of polymer films because the density and level of charge traps are related to the film microstructure [101], [102]. Therefore, higher crystallinity films showed more accumulation of homocharge and lower mobility as well as more deep traps [103].

A Coulomb force caused by effect of the external electric field acts on the molecular chain when charge carriers are captured by the molecular chain with deep traps. Hence the molecules with negative carriers will move toward the anode while the positive carriers move toward the cathode. Trap energy increases with a longer charge retention time as charge stays longer in deep traps than in shallow traps. The effect of Coulomb's force on the molecular chains containing deep traps is increased. Consequently, the accumulation of space charges and distortion of the electric field being more intense within a thick film than in a thin film. In this regard, the molecular weight of polymers plays an important role in determining the film thickness and therefore the amount of space charge accumulation [103], [104]. Anyway, with the growing demand to utilize thin films, the non-destructive space charge measurement methods have evolved over the past years to satisfy the requirements of accuracy and reliability.

The main measurement methods of solid dielectrics have been classified into methods based on mechanical, electrical and thermal disturbance pulses.

The working principle of these methods depends on the displacement of space charge within dielectric by disturbance to generate a displacement current measured by an external circuit [105]. The spatial resolution of conventional mechanical or electrical pulse disturbance-based methods is around several micrometers which causes them unsuited for the space charge measuring of thin films of capacitor-grade. The pulsed electro-acoustic (PEA) method and thermal methods are common methods that have a satisfactory spatial resolution value that can be improved by enhancing measurement accuracy over the surface and internal temperature of the sample.

The PEA method has applied to measure HVDC materials as well as to characterize insulators for DC and AC applications in general and also for the ageing cases [101]. The thermal method has three main types, thermal pulse method (TPM), thermal step method (TSM), and laser intensity modulation method (LIMM). The thermal gradient applied to the sample determines the difference between these types. Anyway, the TP method adopted the time domain to collected available data, it's much faster than the LIMM method which scans the signal in the frequency domain [106], [107].

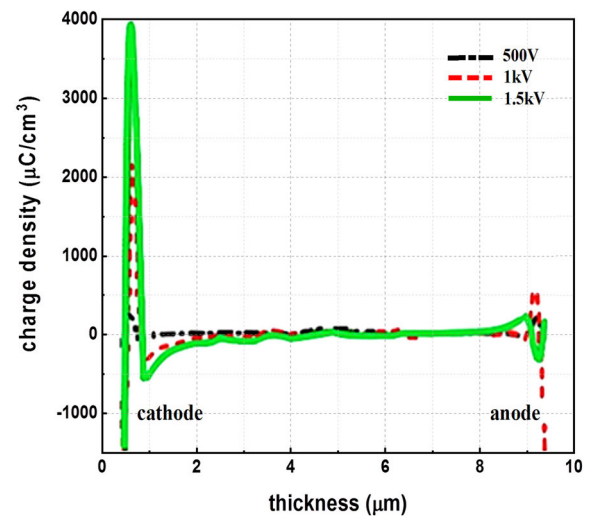


**FIGURE 16.** Space charge distribution characteristics of the BOPP film at 25°C (replotted from [105]).

The polarisation results for a 9.8  $\mu\text{m}$  BOPP film with different DC voltage 0.5, 1, and 1.5 kV, at 25 and 70°C revealed the increasing role of negative charge in injecting of homocharge.

It should be mentioned that the examination of space charge injection and migration within the film was performed under an electric field depending on the improved TP method [108]. At 25°C and under the applied voltage 50 V/ $\mu\text{m}$ , almost no space charge has been detected because this field was less than the threshold field for space charge injection. Upon polarization under the electric fields of 100 and 150 V/ $\mu\text{m}$ , the negative charges were gradually intensified in a region near the cathode surface. The positive charge was formed near to the anode meanwhile, the density of negative charge near the cathode was enhanced under the electrical field of 150 V/ $\mu\text{m}$  (Fig. 16).

The negative charge creates in the deeper bulk of film due to the migration of space charge injected under the effect of high voltage [105]. Where the density and level of the charge trap partially determine the speed of space charge migration within the film. In high electric fields, the trap level changes to be shallow and it becomes easy for the charge to jump from trap to trap, depending on the effect of Poole-Frenkel. It is useful here to point out that the Poole-Frenkel effect has indicated two important factors that can enhance charge injection are the applied field level and temperature. The polarisation under high fields causes the inclination of the energy band-gap because the hole injection needs to get over a higher potential barrier which leads to the injection of asymmetric bipolar space charge [109]. Thus, only the negative charge can be observed in the low electric field, while the injection of positive charge observes at a higher field which leads to more accumulation of asymmetric homo space charges.

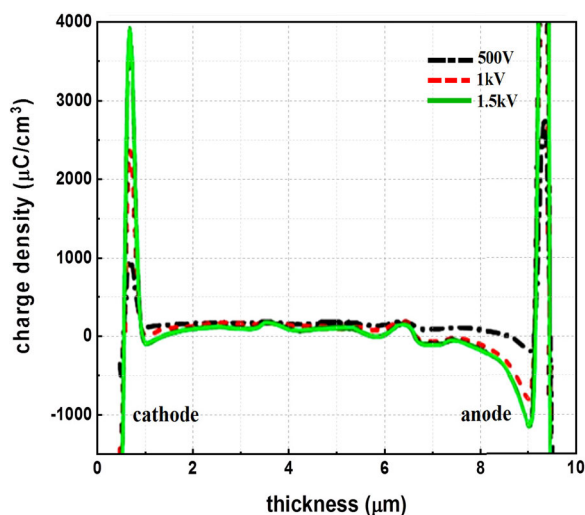


**FIGURE 17.** Space charge distribution characteristics of the BOPP film at 70°C (replotted from [105]).

Under these conditions, the density of negative charge near the anode was much higher than that near the cathode. The effect of the thermal-aided emission is clearly demonstrated through increasing the test temperature, where the negative charge accumulates more and more near the cathode at 70°C, while the polarity of the accumulated charge near the anode oscillates from positive to negative (Fig. 17).

This phenomenon occurs due to dominance of injection of the asymmetric negative charge and the mutual migration of injected charges. However, the high temperature acts to increase the difference in the rate of asymmetric charging injection. Initially, the amount of injected negative space charge was higher than the positive charge. With the increase of the applied voltage influence, the majority of positive charges are overlapped or re-combined with the negative charge during the mutual migration of the injected charge. Ultimately, the high-density heterocharge accumulated adjacent to the anode due to the continuous migrations of numerous negative charges injected [105]. The behavior and effect of the space charge vary in accordance with the type of voltage applied to the dielectric film, as explained by the following.

#### 1) UNDER DC FIELD

Space charge injection with fixed polarity by the electrode weakens the field at the interface and suppresses more space charge injection. At the same time, the field within the material is under the influence of space charges with the same polarity for both sides. Therefore, the breakdown under the influence of DC voltage resulting from space charge accumulation begins damages the material from the inside [37], [110]. The maximum level of the applied DC electrical field distortion on BOPP film due to charge accumulation is 80%. Thus, the accumulated space charge would enhance the ability of PD to cause energy losses and electrical ageing accumulation; as such, the capacitor dielectric lifetime

is shortened [89], [105], [111]. The life of the capacitor dielectric decreases by 2% with each 8°C increment over the temperature range of 40 to 65°C [112].

#### 2) DC WITH AC VOLTAGE

The space charge is injected in the dielectric material at every half cycle, wherein only a small net residual charge accumulates over time. The space charge is highly dependent on frequency: The charge moves deep into the bulk of the sample at a low frequency, whereas the amount of trapped charges increases as frequency decreases [113]. Thus, the amount of the space charge injected under AC voltage is considerably smaller than that stored in the same dielectric under DC voltage with the same root mean square value as the AC voltage [89], [105]. The breakdown under DC stress begins near the bulk of the dielectric, whereas that under AC stress begins near the sample–electrode interface. The electric breakdown strength of the dielectric is low under AC stress and decreases further as the applied frequency is increased in contrast to that under DC breakdown [37].

The amount and behavior of space charges accumulation are related to the frequency of the applied voltage under complex electric fields. The accumulation of space charge decreases and the time required to reach steady-states of charge amount increases with frequency increasing, due to increasing frequent polarity reversals with frequency [113]. The influence of temperature, DC voltage, DC combination voltage and pulse voltage on the surface charge and trapping properties of the PP film has been reported. Detrapping of surface charges from the deep traps can be remarkably enhanced by increasing the temperature [114] thus, the decay of the surface charge is accelerated. Surface charge accumulation is unrelated to temperature under DC voltage, whereas the decay dominates over electric field and temperature. Temperature affects surface charge accumulation by affecting the coupling of surface charges. Coupling complicates surface charge decay under the combination of DC and pulse voltages. Consequently, the electrical field, trap level, and density are asymmetrical with decay under different temperatures [115]. The space charges are resulted by ageing of dielectric materials only, i.e. physical defects (nanocavities) that are formed by field-induced strain are contributing to charges injection [63]. Nanocavities are considerably smaller than microcavities, which are local expansions of the polymer matrix and form in low-density spots in blank places that fill the free volume within molecular chains. Nanocavities are produced under an average field and not under a strong local electric field associated with the accumulation of localised charges; therefore, charge transport and electrical breakdown depend on nanocavity density and size [63], [116], [117]. Polymer ageing is the result of electromechanical stress, and space charge accumulation increases local field and degrades materials via ageing, whilst electrostatic energy increases with field strength to break van der Waals attraction bonds [63], [116], [118].

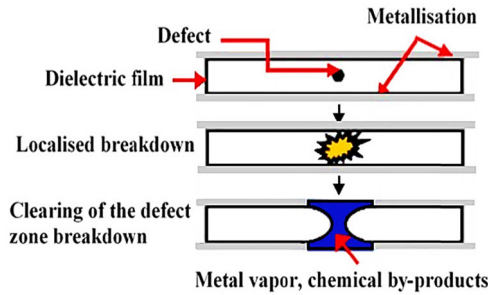


FIGURE 18. Self-healing phenomenon in MPPC (replotted from [15]).

**B. PD AND SELF-HEALIN**

Metallised capacitors have the unique feature of self-healing or clearing, which is the ability to self-repair at the expense of capacitor parameter degradation (graceful failure). Self-healing is a joint process its success depends on metallised layer resistivity and polymer chemical composition. The formation of conductive paths by free carbon in the cleared metallization region at the approximate breakdown site results in poor self-healing and capacitor failure [10], [119]. Defects, impurities or voids in the structure of the crystallised film cause local breakdown under the influence of voltage stress [118], [120]. Thus, PD is attributed to local breakdowns that do not damage the dielectric structure when the local electric field strength exceeds the breakdown resistance of the material (low-density breakdown regions). This process results in the gradual localisation of high temperatures and increases pressure [14], [118]. The dielectric film is punctured during severe discharge, the thin electrode layer at the defect site is rapidly vaporised and driven wards and the site become electrically isolated [15]. Fig.18 illustrates local breakdown or self-healing (clearing).

The basic degradation mechanism of the thin dielectric films caused by PD is illustrated in Fig 19.

The intensity and behavior of the PD vary in accordance with the type of the applied voltage.

**1) UNDER DC VOLTAGE**

Two principal mechanisms affect repetitive PD under the influence of DC voltage. The first is the recharge of dielectric voids via current applied to the dielectric, and the second is the redistribution of charges resulting from discharge [121]. Both processes generate current across voids in the dielectric. The specific changes in DC voltage polarity also affect charge redistribution and PD repetition [121], [122]. The defect related to PD under DC voltage is described by using pulse magnitude and event time [123]. The magnitude of PD greatly depends on the electric field in the cavity at the moment the initiatory electron appears and the discharge process starts. In transient voltage conditions, the voltage across the cavity increases as a result of the high overvoltage which leads to a significant increase in the PD magnitude. Generally, DC discharges have negligible repetition (number of discharges),

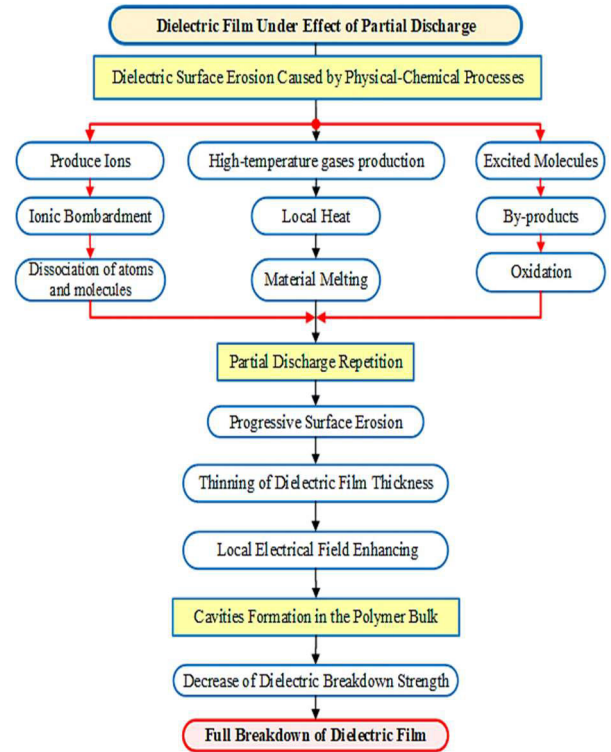


FIGURE 19. Polymer dielectric film degradation due to PD.

small in magnitude and low effective, so the applied voltage is considerably high [124].

**2) UNDER AC VOLTAGE**

Applied AC fields increase the probability of PD accidents with each frequency cycle by redistributing space charge or residual surface charge at a discharge site after each discharge event [125]. As a result, the repetition of PD under AC fields depends on the frequency of applied voltage [126]. High-order harmonics increases the likelihood of PD by increasing voltage at a certain value to block space charge movement and by redistributing the net electric field in defect locations [64]. PD pulses under the influence of AC and DC voltages are clarified in Fig.20 [127], [128].

Comparing the effects of AC and DC voltage on discharge events shows that the amount of discharge under DC voltage is considerably less than that under the AC voltage on the assumption that the dielectric films have the same properties and are subject to the same measurement conditions [49]. The PD events under both AC and DC voltages heavily depend on the film thickness where a void size inside dielectric relates to the random nature of the polymers. Therefore, the biggest void in which an ionization product can reach a sufficient amount of kinetic energy is most likely occurs in the thick film [129]. Anyway, the dielectric films are subjected to high stress under the influence of the superimposed voltage via exposure to voltage ripples and abrupt wave changes that increase the repetition rates of PD with

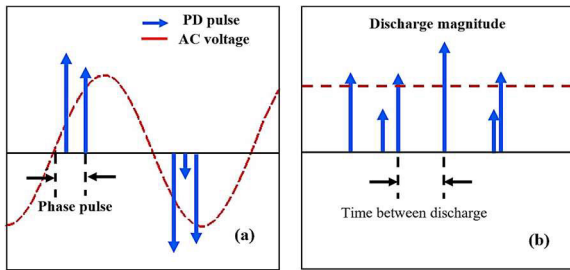


**FIGURE 20.** Pulse repetition characterisation of PD: (a) under AC and (b) under DC electric fields (replotted from [123]).

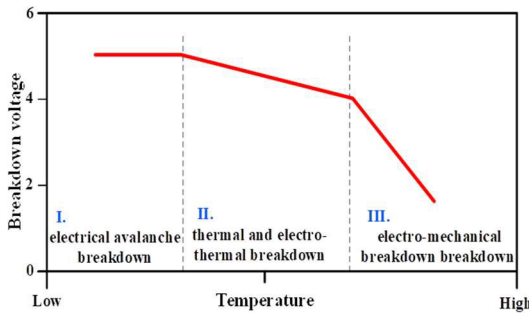


**FIGURE 21.** Overview of polymer dielectric breakdown correlated on temperature with three main breakdown events (replotted from [146]).

increments in ripple frequency; self-healing is consequently enhanced [130], [131]. The increment in self-healing repetition with the continuous weakening of the metal layer results in electrode deterioration via electrochemical corrosion, and the amount of leakage current within the dielectric is increased [123], [130]. Electrochemical corrosion is defined as the gradual change of Al to  $Al_2O_3$  due to the migration of oxygen and/or moisture from a polymer to the metallisation interface; hence, this phenomenon depends on the permeability of the polymer to oxygen and moisture and an electrode interface where the air bubbles are located [10], [130], [132]. Thus, corrosion with ripple current causes the dielectric strength to deteriorate and represents a potential failure mechanism [132], [133].

**V. BREAKDOWN MECHANISMS**

The breakdown of polymer films is a compounded process that is influenced by many factors; often be temperatures, humidity, applied mechanical pressure, film dimension (thickness and area), crystallinity and orientation degrees and electrode quality, and applied voltage type (AC, DC or DC superimposed) [118], [120]. The breakdown occurs as an abrupt phenomenon of the dielectrics leads to lost their functions thus represents lifetime endpoint [16]. This last mechanism which leads to a catastrophic breakdown of a film actually a variety of various complex and conflicting or accumulating processes and their actual source is difficult to be clearly and accurately determined [123], [134]. The external electric field causes a charge of space charge which may lead to negative differential conductivity. Three basic theories to dielectric breakdown: electrical, thermal and mechanical breakdown (Fig. 21).

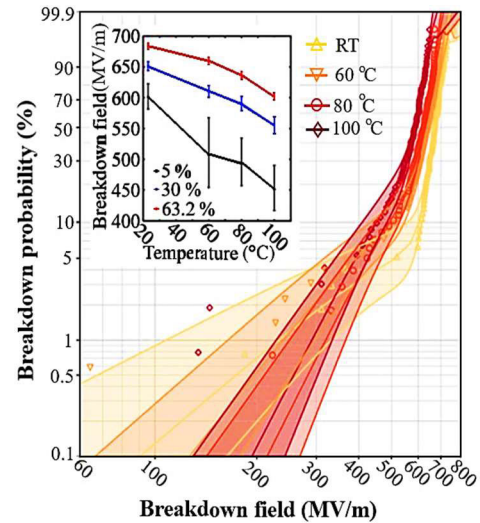


**FIGURE 22.** Characteristics of BOPP breakdown at various temperatures (replotted from [147]).

High temperatures are classified as another factor that affects film breakdown. Breakdown behavior of the capacitor-grade BOPP film with  $6 \mu m$  at different temperatures (RT to  $100 \text{ }^\circ C$ ) was observed using the large-area multi-breakdown method. Test results (Fig. 22) with the partially expanded details of temperatures ranging from  $20 - 100 \text{ }^\circ C$  with percentiles corresponding to breakdown probabilities 5 %, 30 %, and 63.2 % revealed that the Weibull scale parameter tends to decline caused by ageing. The breakdown strength was systematically decreased at 63.2 % from (684 to  $602 \text{ V}/\mu m$ ) for RT to  $100 \text{ }^\circ C$ , respectively. The possibility of multi-breakdown mechanisms depends largely on changes in temperature and dielectric quality. It should be noted that measuring the breakdown of large-area is critical to obtain a realistic perception of dielectric performance. This method allows for the possibility of breakdown measurement regardless of sample weak points, where the defects in the film volume have a significant impact on the formation of the Weibull distribution with increasing area [129].

Film crystallinity also plays a key role factor in the domain of electrical breakdown behavior. The accelerated electro-thermal ageing ( $65 \text{ }^\circ C$  under DC field  $19.2 \text{ V}/\mu m$ ) at 626 hours was performed on the impregnated BOPP films have various crystalline degrees (S1 higher crystalline than S2) with  $6.5 \mu m$  thickness. Measurements of DC voltage breakdown have been performed at ambient temperature  $23 \text{ }^\circ C$  and at 25–30% humidity. The intersection point of the data with the fitted line of 63.2% unreliability line describes the distribution characteristic of the breakdown voltage (1.1kV for S1 film and up to 0.78kV for S2) (Fig 23). Consequently, it can be concluded that the optimum crystallinity of dielectric enhances breakdown strength and contributes to extend film lifetime.

The breakdown usually occurs in most cases as a sudden increase in conduction current followed by the final phase

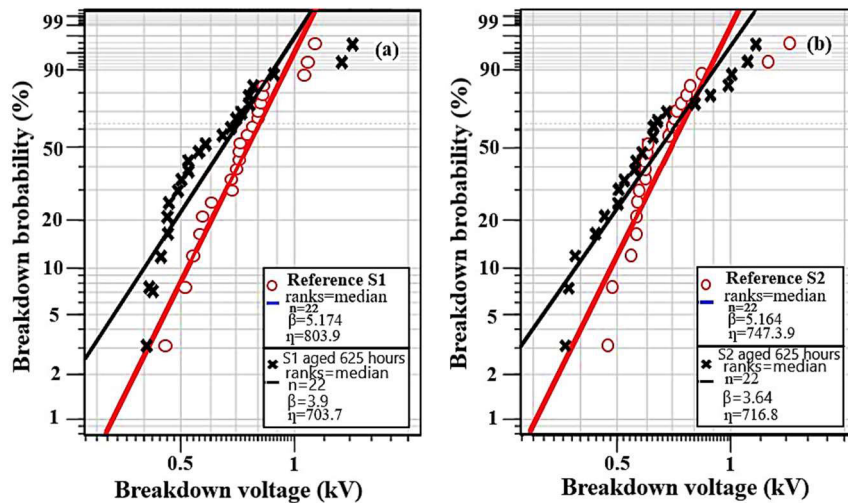


**FIGURE 23.** Weibull distributions of DC breakdown voltage of BOPP films with different crystallisation, (a) S1 and (b) S2 (replotted from [145]).

of electric failure, which is always associated with a thermal tincture [57].

The breakdown mechanism under AC electric field depends on PD behavior, which is determined on the basis of frequency of applied voltage to the film in addition to factors related to film microstructure. Heat accumulation resulting from accelerated PDs activity contributes to the increase of dielectric losses and eventually diminish breakdown strength. Whereas films under DC electric field effect exposed more complex electrical stress; harmonic voltage, transient and over-voltage superposition. Moreover, in cases of parallel DC-capacitors, transient overvoltage occurs at very short time and often with high amplitude, making the dielectric more likely to breakdown [135].

## VI. CONCLUSION

The performance of dielectric films can be efficiently improved by enhancing their ability to withstand DC high voltage levels, temperatures, pulse, and superimposed voltages and harsh working conditions. A comprehensive study and in-depth understanding of the causes and mechanisms of the ageing of capacitor-grade films and methods for developing such dielectrics are needed to meet these requirements. The key points that affect the performance, ageing and development films of MPP capacitors and that require emphasis are summarised as follows:

1. The crystallinity and defects of the BOPP film play a substantial role in determining the electric field threshold, space charge formation, leakage current, and PD events, which are the main factors during the ageing of BOPP films. The crystallinity and defects are related to the microstructure and electrical/mechanical properties of the films during manufacturing and treatment processes and additive ratios.
2. Films defects include on the microcavities, chain bending, dislocating, crystalline and amorphous regions interaction, residual catalyst amount, and antioxidant, besides not completely arranging the molecules regular during the biaxial orientated stretching. In this detail, the effect of nanocavities differs from microcavities, as they are a local extension of the polymer matrix that leads to points of lower density and void spaces filling the free volume between molecular chains. These defects have extremely aggressive interplay with the film surface and they are led to polarisation stem from the space charge, which enhances the electrostatic energy more than coherence energy of BOPP films and makes it at an irreversibly ageing.
3. The electrons hopping distance is highly dependent on the crystallization degree of BOPP film, while temperature increasing stimulates the additional charge carrier mobility to contribute in conduction increases even of the low electric fields. Therefore, the conductance losses increase as a preliminary indicator of thermal ageing.
4. Critical molecular weight limits greatly affect the mechanical properties of BOPP films. These properties are directly responsible for microvoids formation that perform under the influence of increasing stresses to the film chain scission and initiation the PD, ageing and mechanisms of breakdown.
5. The trap levels, migration speed and easily jumping of space charge between traps depend primarily on the high fields applied and /or local fields. High electric field decreasing the energy band of BOPP film, which may lead to more asymmetric injection of bi-polar charge and promote degradation and ageing.
6. Combined thermal, electrical and electro-thermal stresses have devastating effects on the film's reliability

of capacitors. Separating these stresses when investigating ageing, deterioration and breakdown hinders the development of high-voltage DC capacitor films. Hence, research on these mechanisms requires the extensive integration of theoretical and practical aspects.

Although advancements in industrial capacitor industry techniques, a further in-depth research is still required to innovate new methods for the film's production used for high-voltage DC capacitors with excellent ageing resistance, losses, temperature, and energy density.

## REFERENCES

- [1] M. Makdessi, A. Sari, and P. Venet, "Improved model of metallized film capacitors," *IEEE Trans. Dielectrics Electr. Insul.*, vol. 21, no. 2, pp. 582–593, Apr. 2014.
- [2] H. Wang and F. Blaabjerg, "Reliability of capacitors for DC-link applications in power electronic Converters—An overview," *IEEE Trans. Ind. Appl.*, vol. 50, no. 5, pp. 3569–3578, Oct. 2014.
- [3] J. B. Ennis, J. Rauch, X. H. Yang, and J. Atkins, "Comparison of film capacitor designs for a high power density application," in *Proc. IEEE Int. Power Modulator High Voltage Conf.*, May 2010, pp. 225–228.
- [4] T. Umemura and K. Akiyama, "Thermal aging effect on morphology and electrical properties of biaxially oriented polypropylene films," *Electr. Eng. Jpn.*, vol. 105, no. 6, pp. 1–10, 1985.
- [5] J. R. MacDonald, M. A. Schneider, J. B. Ennis, F. W. MacDougall, and X. H. Yang, "High energy density capacitors," *IEEE Electr. Insul., Conf.*, May/Jun. 2009, pp. 306–309.
- [6] J. L. Nash, "Biaxially oriented polypropylene film in power capacitors," *Polym. Eng. Sci.*, vol. 28, no. 13, pp. 862–870, Jul. 1988.
- [7] B. Fan, F. Liu, G. Yang, H. Li, G. Zhang, S. Jiang, and Q. Wang, "Dielectric materials for high-temperature capacitors," *IET Nanodielectrics*, vol. 1, no. 1, pp. 32–40, Apr. 2018.
- [8] A. Wechsler, B. C. Mecrow, D. J. Atkinson, J. W. Bennett, and M. Benarous, "Condition monitoring of DC-link capacitors in aerospace drives," *IEEE Trans. Ind. Appl.*, vol. 48, no. 6, pp. 1866–1874, Nov. 2012.
- [9] W. J. Sarjeant, J. Zirnheld, and F. W. MacDougall, "Capacitors," *IEEE Trans. Plasma Sci.*, vol. 26, no. 5, pp. 1362–1392, Oct. 1998.
- [10] J. Flicker, R. Kaplar, M. Marinella, and J. Granata, "Lifetime testing of metallized thin film capacitors for inverter applications," in *Proc. IEEE 39th Photovoltaic Spec. Conf. (PVSC)*, Jun. 2013, pp. 3340–3341.
- [11] A. Schneuwly, P. Gröning, and L. Schlapbach, "Uncoupling behaviour of current gates in self healing capacitors," *Mater. Sci. Eng., B*, vol. 55, no. 3, pp. 210–220, Sep. 1998.
- [12] R. Blečić, Q. Diduck, and A. Baric, "Minimization of maximum electric field in high-voltage parallel-plate capacitor," in *Proc. 39th Int. Conv. Inf. Commun. Technol., Electron. Microelectron. (MIPRO)*, May 2016, pp. 99–103.
- [13] J. Lehr, and P. Ron, *Foundations of Pulsed Power Technology, Power Technology and Power Engineering*. Hoboken, NJ, USA: Wiley, 2017.
- [14] M. H. El-Husseini, P. Venet, G. Rojart, and M. Fathallah, "Effect of the geometry on the aging of metallized polypropylene film capacitors," in *Proc. IEEE 32nd Annu. Power Electron. Specialists Conf.*, Jun. 2001, pp. 2061–2066.
- [15] M. Makdessi, A. Sari, and P. Venet, "Metallized polymer film capacitors ageing law based on capacitance degradation," *Microelectron. Rel.*, vol. 54, nos. 9–10, pp. 1823–1827, Sep. 2014.
- [16] J. C. Fothergill, "Ageing, space charge and nanodielectrics: Ten things we don't know about dielectrics," in *Proc. IEEE Int. Conf. Solid Dielectrics*, Jul. 2007, pp. 1–10.
- [17] G. C. Montanari and L. Simoni, "Aging phenomenology and modeling," *IEEE Trans. Electr. Insul.*, vol. 28, no. 5, pp. 755–776, Oct. 1993.
- [18] G. Mazzanti, G. C. Montanari, and L. A. Dissado, "Elemental strain and trapped space charge in thermoelectrical aging of insulating materials: Life modeling," *IEEE Trans. Dielectrics Electr. Insul.*, vol. 8, no. 6, pp. 966–971, Dec. 2001.
- [19] L. Qi, L. Petersson, and T. Liu, "Review of recent activities on dielectric films for capacitor applications," *J. Int. Council Electr. Eng.*, vol. 4, no. 1, pp. 1–6, Sep. 2014.
- [20] I. Rytöluoto, A. Gitsas, S. Pasanen, and K. Lahti, "Effect of film structure and morphology on the dielectric breakdown characteristics of cast and biaxially oriented polypropylene films," *Eur. Polym. J.*, vol. 95, pp. 606–624, Oct. 2017.
- [21] A. Kahouli, O. Gallot-Lavallée, P. Rain, O. Lesaint, L. Heux, C. Guillermin, and J.-M. Lupin, "Structure effect of thin film polypropylene view by dielectric spectroscopy and X-ray diffraction: Application to dry type power capacitors," *J. Appl. Polym. Sci.*, vol. 132, no. 39, Jun. 2015.
- [22] M. Rabuffi and G. Picci, "Status quo and future prospects for metallized polypropylene energy storage capacitors," *IEEE Trans. Plasma Sci.*, vol. 30, no. 5, pp. 1939–1942, Oct. 2002.
- [23] S. Laihonon, U. Gafvert, T. Schutte, and U. Gedde, "DC breakdown strength of polypropylene films: Area dependence and statistical behavior," *IEEE Trans. Dielectrics Electr. Insul.*, vol. 14, no. 2, pp. 275–286, Apr. 2007.
- [24] C. Yu, Q. Xie, Y. Bao, G. Shan, and P. Pan, "Crystalline and spherulitic morphology of polymers crystallized in confined systems," *Crystals*, vol. 7, no. 5, p. 147, May 2017.
- [25] E. M. Troisi, H. J. M. Caelers, and G. W. M. Peters, "Full characterization of multiphase, multimorphological kinetics in flow-induced crystallization of IPP at elevated pressure," *Macromolecules*, vol. 50, no. 10, pp. 3868–3882, May 2017.
- [26] Q. Liu, X. Sun, H. Li, and S. Yan, "Orientation-induced crystallization of isotactic polypropylene," *Polymer*, vol. 54, no. 17, pp. 4404–4421, Aug. 2013.
- [27] X. Shen, W. Hu, and T. P. Russell, "Measuring the degree of crystallinity in semicrystalline regioregular Poly(3-hexylthiophene)," *Macromolecules*, vol. 49, no. 12, pp. 4501–4509, Jun. 2016.
- [28] T. Wu, M. Xiang, Y. Cao, J. Kang, and F. Yang, "Pore formation mechanism of nucleated  $\beta$  polypropylene stretched membranes," *RSC Adv.*, vol. 4, no. 69, pp. 36689–36701, 2014.
- [29] G. T. Offord, S. R. Armstrong, B. D. Freeman, E. Baer, A. Hiltner, and D. R. Paul, "Influence of processing strategies on porosity and permeability of  $\beta$  nucleated isotactic polypropylene stretched films," *Polymer*, vol. 54, no. 11, pp. 2796–2807, May 2013.
- [30] S. Tamura, K. Ohta, and T. Kanai, "Study of crater structure formation on the surface of biaxially oriented polypropylene film," *J. Appl. Polym. Sci.*, vol. 124, no. 4, pp. 2725–2735, 2012.
- [31] M. T. Demeuse, *Biaxial Stretching of Film: Principles and Applications*. Amsterdam, The Netherlands: Elsevier, 2011.
- [32] X. Qi, Z. Zheng, and S. Boggs, "Computation of electro-thermal breakdown of polymer films," in *Proc. Annu. Rep. Conf. Electr. Insul. Dielectric Phenomena*, Albuquerque, NM, USA, Oct. 2003, pp. 337–340.
- [33] V. Dua, "Analysis of charge rigidity properties in polymer films with halogen treatment," *Int. Ref. J. Eng. Sci.*, vol. 7, no. 1, pp. 47–53, 2018.
- [34] M. Xiao and B. X. Du, "Review of high thermal conductivity polymer dielectrics for electrical insulation," *High Voltage*, vol. 1, no. 1, pp. 34–42, Apr. 2016.
- [35] X. Yuan and T. C. M. Chung, "Cross-linking effect on dielectric properties of polypropylene thin films and applications in electric energy storage," *Appl. Phys. Lett.*, vol. 98, no. 6, Feb. 2011, Art. no. 062901.
- [36] S. Diahm, M. Bechara, M.-L. Locatelli, R. Khazaka, C. Tenailleau, and R. Kumar, "Dielectric strength of parylene HT," *J. Appl. Phys.*, vol. 115, no. 5, Feb. 2014, Art. no. 054102.
- [37] S. Li, Y. Zhu, D. Min, and G. Chen, "Space charge modulated electrical breakdown," *Sci. Rep.*, vol. 6, no. 1, p. 32588, Sep. 2016.
- [38] L. Capt, "Simultaneous biaxial stretching of isotactic polypropylene films in the partly molten state," Ph.D. dissertation, Dept. Chem. Eng., McGill Univ., Montreal, QC, Canada, 2003.
- [39] K. Wu, T. Okamoto, and Y. Suzuoki, "Simulation study on the correlation between morphology and electrical breakdown in polyethylene," *J. Appl. Phys.*, vol. 98, no. 11, Dec. 2005, Art. no. 114102.
- [40] X. Qiu, W. Wirges, R. Gerhard, M. Ren, M. Tefferi, and Y. Cao, "Electrical-insulation behavior of cellular polymer foams in comparison to their piezoelectric properties," in *Proc. IEEE Int. Conf. High Voltage Eng. Appl. (ICHVE)*, Sep. 2016, pp. 1–4.
- [41] L.-P. Meng, X.-W. Chen, Y.-F. Lin, and L.-B. Li, "Improving the softness of BOPP films: From laboratory investigation to industrial processing," *Chin. J. Polym. Sci.*, vol. 35, no. 9, pp. 1122–1131, Jul. 2017.

- [42] A. Menyhard, P. Suba, Z. Laszlo, H. M. Fekete, A. O. Mester, Z. Horvath, G. Voros, J. Varga, and J. Moczó, "Direct correlation between modulus and the crystalline structure in isotactic polypropylene," *Express Polym. Lett.*, vol. 9, no. 3, pp. 308–320, 2015.
- [43] R. A. C. Deblieck, D. J. M. van Beek, K. Remerie, and I. M. Ward, "Failure mechanisms in polyolefines: The role of crazing, shear yielding and the entanglement network," *Polymer*, vol. 52, no. 14, pp. 2979–2990, Jun. 2011.
- [44] Z. Bartczak and A. Galeski, "Mechanical properties of polymer blends," in *Polymer Blends Handbook*, L. Utracki and C. Wilkie, Eds. Dordrecht, The Netherlands: Springer, 2014, pp. 1203–1297.
- [45] Y. Yamamoto, M. Asano, H. Yoshida, M. Kobayashi, and H. Toda, "Effect of micro-voids on crack initiation and propagation in bending deformation of Al-Mg-Si alloy sheet," *Mater. Sci. Forum*, vols. 794–796, pp. 325–330, Jun. 2014.
- [46] L. A. Utracki and C. Wilkie, *Polymer Blends Handbook* (Polymer Science), 2nd ed. Dordrecht, The Netherlands: Springer, 2014, pp. 123–201.
- [47] Z. Bartczak, A. S. Argon, R. E. Cohen, and M. Weinberg, "Toughness mechanism in semi-crystalline polymer blends: II. High-density polyethylene toughened with calcium carbonate filler particles," *Polymer*, vol. 40, no. 9, pp. 2347–2365, Apr. 1999.
- [48] E. J. Clark, "Molecular and microstructural factors affecting mechanical properties of polymeric cover plate materials," Center Building Technol., Nat. Bureau Standards, Washington, DC, USA, 1985, pp. 27–45.
- [49] I. Amer, A. van Reenen, and T. Mokrani, "Molecular weight and tacticity effect on morphological and mechanical properties of Ziegler–Natta catalyzed isotactic polypropylenes," *Polímeros*, vol. 25, no. 6, pp. 556–563, Dec. 2015.
- [50] M. Kutz, *Mechanical Engineer's Handbook* (Materials and Engineering Mechanics), vol. 1. Hoboken, NJ, USA: Wiley, 2015.
- [51] C. Bendjaouahdou and S. Bensaad, "Aging studies of a polypropylene and natural rubber blend," *Int. J. Ind. Chem.*, vol. 9, no. 4, pp. 345–352, Dec. 2018.
- [52] J. Pospisil, Z. Horák, J. Pilar, N. C. Billingham, H. Zweifel, and S. Nespurek, "Influence of testing conditions on the performance and durability of polymer stabilisers in thermal oxidation," *Polym. Degradation Stability*, vol. 82, no. 2, pp. 145–162, Jan. 2003.
- [53] A. Law, L. Simon, and P. Lee-Sullivan, "Effects of thermal aging on isotactic polypropylene crystallinity," *Polym. Eng. Sci.*, vol. 48, no. 4, pp. 627–633, 2008.
- [54] J. Zhang, F. Wang, J. Li, H. Ran, X. Li, and Q. Fu, "Breakdown voltage and its influencing factors of thermally aged oil-impregnated paper at pulsating DC voltage," *Energies*, vol. 10, no. 9, p. 1411, Sep. 2017.
- [55] M. E. Stournara and R. Ramprasad, "A first principles investigation of isotactic polypropylene," *J. Mater. Sci.*, vol. 45, no. 2, pp. 443–447, Jan. 2010.
- [56] A. Huzayyin, S. Boggs, and R. Ramprasad, "Density functional analysis of chemical impurities in dielectric polyethylene," *IEEE Trans. Dielectrics Electr. Insul.*, vol. 17, no. 3, pp. 926–930, Jun. 2010.
- [57] L. A. Dissado and J. C. Fothergil, *Electrical Degradation and Breakdown in Polymers*, vol. 9. London, U.K.: IET, 1992.
- [58] J. McPherson, J. Kim, A. Shanware, H. Mogul, and J. Rodriguez, "Proposed universal relationship between dielectric breakdown and dielectric constant," in *IEDM Tech. Dig.*, Dec. 2002, pp. 633–636.
- [59] H.-V. Nguyen and T. H. Pham, "Structural and electronic properties of defect-free and defect-containing polypropylene: A computational study by van der Waals density-functional method," *Phys. Status Solidi (B)*, vol. 255, no. 3, Oct. 2017, Art. no. 1700036.
- [60] Q. Gao, Y. Liu, Y. Gao, B. X. Du, Q. Wang, H. Liu, and K. Ye, "Effects of charging/discharging cycles on breakdown characteristics of polypropylene film," in *Proc. IEEE 2nd Int. Conf. Dielectrics (ICD)*, Jul. 2018, pp. 1–4.
- [61] C. A. Bishop and G. Tullo, "How items such as dust, oligomers & slip agents can affect the polymer lm surface quality and be potential problems in high-tech roll-to-roll vacuum deposition applications," in *Proc. Annu. Tech. Conf. Soc. Vacuum, Coaters*, Raleigh, NC, USA, 2006, pp. 648–653.
- [62] T. Umemura, K. Abe, K. Akiyama, and D. Couderc, "Thermal-aging behavior of bo-pp films," *IEEE Trans. Electr. Insul.*, vol. EI-22, no. 6, pp. 735–743, Dec. 1987.
- [63] J.-P. Crine, "On the interpretation of some electrical aging and relaxation phenomena in solid dielectrics," *IEEE Trans. Dielectrics Electr. Insul.*, vol. 12, no. 6, pp. 1089–1107, Dec. 2005.
- [64] J. Ho and T. R. Jow, "High field conduction in biaxially oriented polypropylene at elevated temperature," *IEEE Trans. Dielectrics Electr. Insul.*, vol. 19, no. 3, pp. 990–995, Jun. 2012.
- [65] G. M. Treich, S. Nasreen, A. Mannodi Kanakkithodi, R. Ma, M. Tefferi, J. Flynn, Y. Cao, R. Ramprasad, and G. A. Sozning, "Optimization of organotin polymers for dielectric applications," *ACS Appl. Mater. Interfaces*, vol. 8, no. 33, pp. 21270–21277, Aug. 2016.
- [66] D. M. Mowery, R. L. Clough, and R. A. Assink, "Identification of oxidation products in selectively labeled polypropylene with solid-State <sup>13</sup>C NMR techniques," *Macromolecules*, vol. 40, no. 10, pp. 3615–3623, May 2007.
- [67] G. Zhang, C. Nam, L. Petersson, J. Jämbeck, H. Hillborg, and T. C. M. Chung, "Increasing polypropylene high temperature stability by blending polypropylene-bonded hindered phenol antioxidant," *Macromolecules*, vol. 51, no. 5, pp. 1927–1936, Feb. 2018.
- [68] A. C. Kolbert, J. G. Didier, and L. Xu, "Mechanochemical degradation of ethylene–Propylene copolymers: Characterization of olefin chain ends," *Macromolecules*, vol. 29, no. 27, pp. 8591–8598, Jan. 1996.
- [69] C. D. Cook and R. C. Woodworth, "Oxidation of hindered Phenols. II. the 2,4,6-tri-*t*-butylphenoxy radical," *J. Amer. Chem. Soc.*, vol. 75, no. 24, pp. 6242–6244, Dec. 1953.
- [70] M. M. Murzakanova, T. A. Borukaev, M. M. Begretov, and A. K. Mikitaev, "The degradation of polyethylene and mechanisms of its stabilisation by azomethinephenylmelamine compounds," *Int. Polym. Sci. Technol.*, vol. 41, no. 11, pp. 43–48, Sep. 2018.
- [71] G. Zografí and A. Newman, "Interrelationships between structure and the properties of amorphous solids of pharmaceutical interest," *J. Pharmaceutical Sci.*, vol. 106, no. 1, pp. 5–27, Jan. 2017.
- [72] T. G. Ryan and P. D. Calvert, "Diffusion and annealing in crystallizing polymers," *Polymer*, vol. 23, no. 6, pp. 877–883, Jun. 1982.
- [73] S. B. Aziz, T. J. Woo, M. F. Z. Kadir, and H. M. Ahmed, "A conceptual review on polymer electrolytes and ion transport models," *J. Sci., Adv. Mater. Devices*, vol. 3, no. 1, pp. 1–17, Mar. 2018.
- [74] B. Dellinger, S. Lomnicki, L. Khachatryan, Z. Maskos, R. W. Hall, J. Adoukpe, C. McFerrin, and H. Truong, "Formation and stabilization of persistent free radicals," *Proc. Combustion Inst.*, vol. 31, no. 1, pp. 521–528, Jan. 2007.
- [75] K. Uchida and N. Shimizu, "The effect of temperature and voltage on polymer chain scission in high-field region," *IEEE Trans. Electr. Insul.*, vol. 26, no. 2, pp. 271–277, Apr. 1991.
- [76] M. Rjeb, A. Labzour, A. Rjeb, S. Sayouri, Y. Claire, and A. Périchaud, "TG and DSC studies of natural and artificial aging of polypropylene," *Phys. A, Stat. Mech. Appl.*, vol. 358, no. 1, pp. 212–217, Dec. 2005.
- [77] W. L. Oliani, D. M. Fermino, L. F. C. P. de Lima, A. B. Lugao, and D. F. Parra, "Effects of accelerated thermal aging on polypropylene modified by irradiation process," in *Characterization of Minerals, Metals, and Materials*. Cham, Switzerland: Springer, 2015, pp. 651–658.
- [78] J. F. Rubinson and Y. P. Kayinamura, "Charge transport in conducting polymers: Insights from impedance spectroscopy," *Chem. Soc. Rev.*, vol. 38, no. 12, p. 3339, 2009.
- [79] T. D. Huan, S. Boggs, G. Teyssedre, C. Laurent, M. Cakmak, S. Kumar, and R. Ramprasad, "Advanced polymeric dielectrics for high energy density applications," *Progr. Mater. Sci.*, vol. 83, pp. 236–269, Oct. 2016.
- [80] I. Rytoluoto, M. Ritamaki, and K. Lahti, "Short-term dielectric performance assessment of BOPP capacitor films: A baseline study," in *Proc. 12th Int. Conf. Properties Appl. Dielectric Mater. (ICPADM)*, May 2018, pp. 289–292.
- [81] A. Thielen, J. Niezette, G. Feyder, and J. Vanderschueren, "Thermally stimulated current study of space charge formation and contact effects in metal-polyethylene terephthalate film-metal systems. I. Generalities and theoretical model," *J. Phys. Chem. Solids*, vol. 57, no. 11, pp. 1567–1580, Nov. 1996.
- [82] J. R. Dennison and J. Brunson, "Temperature and electric field dependence of conduction in low-density polyethylene," *IEEE Trans. Plasma Sci.*, vol. 36, no. 5, pp. 2246–2252, Oct. 2008.
- [83] H. Li, Z. Li, Z. Xu, F. Lin, B. Wang, H. Li, Q. Zhang, W. Wang, and X. Huang, "Electric field and temperature dependence of electrical conductivity in biaxially oriented polypropylene films," *IEEE Trans. Plasma Sci.*, vol. 42, no. 11, pp. 3585–3591, Nov. 2014.
- [84] H. Jiang, L. Hong, N. Venkatasubramanian, J. T. Grant, K. Eyink, K. Wiecek, S. Fries-Carr, J. Enlow, and T. J. Bunning, "The relationship between chemical structure and dielectric properties of plasma-enhanced chemical vapor deposited polymer thin films," *Thin Solid Films*, vol. 515, nos. 7–8, pp. 3513–3520, Feb. 2007.

- [85] J. D. Mendelsohn, C. J. Barrett, V. V. Chan, A. J. Pal, A. M. Mayes, and M. F. Rubner, "Fabrication of microporous thin films from poly-electrolyte multilayers," *Langmuir*, vol. 16, no. 11, pp. 5017–5023, May 2000.
- [86] T. Yamamoto, "Computer modeling of polymer crystallization—Toward computer-assisted materials' design," *Polymer*, vol. 50, no. 9, pp. 1975–1985, Apr. 2009.
- [87] Y. Hayase, T. Osada, T. Takada, and Y. Tanaka, "Numerical estimation of trap depth in polymeric materials using molecular orbital method," in *Proc. IEEE Conf. Electr. Insul. Dielectric Phenomena*, Virginia Beach, VA, USA, Aug. 2009, pp. 161–164.
- [88] V. A. Zakrevskii, N. T. Sudar, A. Zaopo, and Y. A. Dubitsky, "Mechanism of electrical degradation and breakdown of insulating polymers," *J. Appl. Phys.*, vol. 93, no. 4, pp. 2135–2139, Feb. 2003.
- [89] H. Li, L. Li, L. Li, W. Wang, X. Huang, Q. Chen, and F. Lin, "Study on the impact of space charge on the lifetime of pulsed capacitors," *IEEE Trans. Dielectrics Electr. Insul.*, vol. 24, no. 3, pp. 1870–1877, Jun. 2017.
- [90] P. D. Bastidas and S. M. Rowland, "Interfacial aging in composite insulators as a result of partial discharge activity," in *Proc. IEEE Electr. Insul. Conf. (EIC)*, Jun. 2017, pp. 13–16.
- [91] G. Wilson, J. R. Dennison, A. E. Jensen, and J. Dekany, "Electron energy-dependent charging effects of multilayered dielectric materials," *IEEE Trans. Plasma Sci.*, vol. 41, no. 12, pp. 3536–3544, Dec. 2013.
- [92] W. Zhao, W. H. Siew, M. J. Given, Q. Li, J. He, and E. Corr, "Aging behaviour of polypropylene under various voltage stresses," in *Proc. IEEE Conf. Electr. Insul. Dielectric Phenomena (CEIDP)*, Oct. 2016, pp. 903–906.
- [93] W. Zhao, W. H. Siew, M. J. Given, Q. Li, J. He, and E. Corr, "Thermoplastic materials aging under various stresses," in *Proc. IEEE Electr. Insul. Conf. (EIC)*, Jun. 2016, pp. 615–618.
- [94] I. Plesa, P. V. Notingher, S. Schlögl, C. Sumereder, and M. Muhr, "Properties of polymer composites used in high-voltage applications," *Polymers*, vol. 8, no. 5, p. 173, Apr. 2016.
- [95] L. A. Dissado, C. Laurent, G. C. Montanari, and P. H. F. Morshuis, "Demonstrating a threshold for trapped space charge accumulation in solid dielectrics under DC field," *IEEE Trans. Dielectrics Electr. Insul.*, vol. 12, no. 3, pp. 612–620, Jun. 2005.
- [96] J. Di, W.-J. Mei, W.-L. Pan, G.-H. Song, and X.-L. Qin, "The influence of space charge on the insulation failure of DC cable and its mechanism study," in *Proc. 3rd Annu. Int. Conf. Adv. Mater. Eng. (AME)*. Shanghai, China: Atlantis Press, 2017.
- [97] F. Zheng, C. Lin, C. Liu, Z. An, Q. Lei, and Y. Zhang, "A method to observe fast dynamic space charge in thin dielectric films," *Appl. Phys. Lett.*, vol. 101, no. 17, Oct. 2012, Art. no. 172904.
- [98] A. Santos, "Deep and shallow core excitation and ionization of atoms and molecules," *Int. J. Experim. Spectroscopic Techn.*, vol. 3, no. 2, pp. 1–13, Oct. 2018.
- [99] M. H. Lean and W.-P. L. Chu, "Simulation of charge packet formation in layered polymer film," *COMPEL-Int. J. Comput. Math. Electr. Electron. Eng.*, vol. 33, no. 4, pp. 1396–1415, Jul. 2014.
- [100] G. C. Montanari, "Relation between space charge and polymeric insulation ageing: Cause and effect," *IEE Proc.-Sci., Meas. Technol.*, vol. 150, no. 2, pp. 53–57, Mar. 2003.
- [101] F. Zheng, M. Gu, J. Dong, Z. An, Q. Lei, and Y. Zhang, "Fast space charge behavior in heat-treated polypropylene films," *J. Appl. Polym. Sci.*, vol. 132, no. 28, Apr. 2015.
- [102] T. Mizutani, "Effects of additives and morphology on space charge in LDPE," in *Proc. Int. Symp. Electr. Insulating Mater. (ISEIM) . Asian Conf. Electr. Insulating Diagnosis (ACEID)*, 33rd Symp. Electr. Ele, Himeji, Japan, Nov. 2001, pp. 487–492.
- [103] Y. Zhang, T. Christen, X. Meng, J. Chen, and J. Rocks, "Research progress on space charge characteristics in polymeric insulation," *J. Adv. Dielectrics*, vol. 6, no. 1, Apr. 2016, Art. no. 1630001.
- [104] D. Min, Y. Li, C. Yan, D. Xie, S. Li, Q. Wu, and Z. Xing, "Thickness-dependent DC electrical breakdown of polyimide modulated by charge transport and molecular displacement," *Polymers*, vol. 10, no. 9, p. 1012, Sep. 2018.
- [105] F. Zheng, Y. Miao, J. Dong, Z. An, Q. Lei, and Y. Zhang, "Space charge characterization in biaxially oriented polypropylene films," *IEEE Trans. Dielectrics Electr. Insul.*, vol. 23, no. 5, pp. 3102–3107, Oct. 2016.
- [106] A. Mellinger, R. Singh, and R. Gerhard-Multhaupt, "Fast thermal-pulse measurements of space-charge distributions in electret polymers," *Rev. Sci. Instrum.*, vol. 76, no. 1, Jan. 2005, Art. no. 013903.
- [107] A. Imburgia, R. Miceli, E. R. Sanseverino, P. Romano, and F. Viola, "Review of space charge measurement systems: Acoustic, thermal and optical methods," *IEEE Trans. Dielectrics Electr. Insul.*, vol. 23, no. 5, pp. 3126–3142, Oct. 2016.
- [108] F. Zheng, C. Liu, C. Lin, Z. An, Q. Lei, and Y. Zhang, "Thermal pulse measurements of space charge distributions under an applied electric field in thin films," *Meas. Sci. Technol.*, vol. 24, no. 6, Apr. 2013, Art. no. 065603.
- [109] K. C. Kao *Dielectric Phenomena in Solids*. San Diego, CA, USA: Elsevier, 2004, pp. 381–509.
- [110] M. Fujii, M. Fukuma, T. Tokoro, Y. Muramoto, N. Hozumi, and M. Nagao, "Numerical analysis of space charge distribution in polypropylene film under AC high field," in *Proc. Int. Symp. Electr. Insulating Mater. (ISEIM) . Asian Conf. Electr. Insulating Diagnosis (ACEID)*, 33rd Symp. Electr. Ele, Nov. 2001, pp. 156–159.
- [111] G. C. Montanari, "Bringing an insulation to failure: The role of space charge," *IEEE Trans. Dielectr. Electr. Insul.*, vol. 18, no. 2, pp. 339–364, Mar. 2011.
- [112] Z. Li, H. Li, X. Huang, H. Li, W. Wang, B. Wang, F. Lin, and Q. Zhang, "Temperature rise of metallized film capacitors in repetitive pulse applications," *IEEE Trans. Plasma Sci.*, vol. 43, no. 6, pp. 2038–2045, Jun. 2015.
- [113] C. Zhou and G. Chen, "The influence of frequency of AC component on space charge behaviours in polyethylene under combined AC and DC electric fields," in *Proc. IEEE Conf. Electr. Insul. Dielectric Phenomena (CEIDP)*, Oct. 2014, pp. 852–855.
- [114] L. Lan, J. Wu, Y. Yin, X. Li, and Z. Li, "Effect of temperature on space charge trapping and conduction in cross-linked polyethylene," *IEEE Trans. Dielectrics Electr. Insul.*, vol. 21, no. 4, pp. 1784–1791, Aug. 2014.
- [115] B. X. Du, W. B. Zhu, J. Li, Y. Q. Xing, and P. H. Huang, "Temperature-dependent surface charge behavior of polypropylene film under DC and pulse voltages," *IEEE Trans. Dielectrics Electr. Insul.*, vol. 24, no. 2, pp. 774–783, Apr. 2017.
- [116] T. Mizutani, H. Semi, and K. Kaneko, "Space charge behavior in low-density polyethylene," *IEEE Trans. Dielectrics Electr. Insul.*, vol. 7, no. 4, pp. 503–508, Aug. 2000.
- [117] W. Brandt and J. Wilkenfeld, "Electric field dependence of positronium formation in condensed matter," *Phys. Rev. B*, vol. 12, no. 7, pp. 2579–2587, Oct. 1975.
- [118] S. Ul Haq and G. G. Raju, "DC breakdown characteristics of high temperature polymer films," *IEEE Trans. Dielectrics Electr. Insul.*, vol. 13, no. 4, pp. 917–926, Aug. 2006.
- [119] J. S. Ho and S. G. Greenbaum, "Polymer capacitor dielectrics for high temperature applications," *ACS Appl. Mater. Inter.*, vol. 10, no. 35, pp. 29189–29218, Aug. 2018.
- [120] M. S. Naidu, and V. Kamaraju, *High Voltage Engineering, Electrical Engineering*. New York, NY, USA: McGraw-Hill, 1996.
- [121] P. Morshuis, M. Jeroense, and J. Beyer, "Partial discharge. Part XXIV: The analysis of PD in HVDC equipment," *IEEE Elect. Insul. Mag.*, vol. 13, no. 2, pp. 6–16, Mar. 1997.
- [122] P. H. F. Morshuis and J. J. Smit, "Partial discharges at DC voltage: Their mechanism, detection and analysis," *IEEE Trans. Dielectrics Electr. Insul.*, vol. 12, no. 2, pp. 328–340, Apr. 2005.
- [123] M. A. Fard, A. J. Reid, and D. M. Hepburn, "Analysis of HVDC superimposed harmonic voltage effects on partial discharge behavior in solid dielectric media," *IEEE Trans. Dielectrics Electr. Insul.*, vol. 24, no. 1, pp. 7–16, Feb. 2017.
- [124] E. A. Morris and W. H. Siew, "Partial discharge activity in polymeric cable insulation under high voltage AC and DC," in *Proc. 52nd Int. Universities Power Eng. Conf. (UPEC)*, Aug. 2017, pp. 1–4.
- [125] Y. Z. Arief, W. A. Izzati, and Z. Adzis, "Modeling of partial discharge mechanisms in solid dielectric material," *Int. J. Eng. Innov. Tech.*, vol. 1, no. 4, pp. 1–6, 2012.
- [126] P. K. Olsen, I. R. Velo, and F. Mauseth, "Experimental challenges when measuring partial discharges under combined DC and high frequency AC voltage," in *Proc. Nordic Insul. Symp.*, vol. 24, Sep. 2017, pp. 86–91.
- [127] C. A. Balanis, *Advanced Engineering Electromagnetics, Electromagnetic Theory*, 2nd ed. Hoboken, NJ, USA: Wiley, 2012.
- [128] U. Fromm and E. Gulski, "Statistical behavior of internal partial discharges at DC Voltage," *Jpn. J. App. Phys.*, vol. 33, no. 12R, p. 6708, 1994.
- [129] K. Theodosiou, D. P. Agoris, I. Gialas, and I. Vitellas, "Measurements of partial discharges and power losses in pet films in high voltage AC fields," *J. Electr. Eng., Bratis.*, vol. 58, no. 5, pp. 250–256, 2007.

- [130] H. Li, Y. Chen, F. Lin, B. Peng, F. Lv, M. Zhang, and Z. Li, "The capacitance loss mechanism of metallized film capacitor under pulsed discharge condition," *IEEE Trans. Dielectrics Electr. Insul.*, vol. 18, no. 6, pp. 2089–2094, Dec. 2011.
- [131] R. Bever and J. Westrom, "Partial discharge testing under direct voltage conditions," *IEEE Trans. Aerosp. Electron. Syst.*, vol. AES-18, no. 1, pp. 82–93, Jan. 1982.
- [132] M. Makdessi, A. Sari, P. Venet, P. Bevilacqua, and C. Joubert, "Accelerated ageing of metallized film capacitors under high ripple currents combined with a DC voltage," *IEEE Trans. Power Electron.*, vol. 30, no. 5, pp. 2435–2444, May 2015.
- [133] H. Li, P. Lewin, and J. C. Fothergill, "Aging mechanisms of X2 metallized film capacitors in a high temperature and humidity environment," in *Proc. IEEE Int. Conf. Dielectrics (ICD)*, vol. 2, Jul. 2016, pp. 804–807.
- [134] M. Ieda, "Dielectric breakdown process of polymers," *IEEE Trans. Electr. Insul.*, vol. EI-15, no. 3, pp. 206–224, Jun. 1980.
- [135] W. Khachen, J. R. Laghari, and W. J. Sarjeant, "Dielectric breakdown of polypropylene under high frequency fields," in *Proc. Conf. Rec. IEEE Int. Symp. Electr. Insul.*, Jun. 1992, pp. 185–188.
- [136] P. A. O'Connell, M. J. Bonner, R. A. Duckett, and I. M. Ward, "The relationship between slow crack propagation and tensile creep behaviour in polyethylene," *Polymer*, vol. 36, no. 12, pp. 2355–2362, Jan. 1995.
- [137] P. A. O'Connell, R. A. Duckett, and I. M. Ward, "Brittle-ductile transitions in polyethylene," *Polym. Eng. Sci.*, vol. 42, no. 7, pp. 1493–1508, Apr. 2004.
- [138] M. M. Caruso, D. A. Davis, Q. Shen, S. A. Odom, N. R. Sottos, S. R. White, and J. S. Moore, "Mechanically-induced chemical changes in polymeric materials," *Chem. Rev.*, vol. 109, no. 11, pp. 5755–5798, Nov. 2009.
- [139] P. Mach, M. Horak, and C. Stancu, "Thermal ageing of polypropylene film capacitors," in *Proc. 38th Int. Spring Seminar Electron. Technol. (ISSE)*, May 2015, pp. 272–276.
- [140] J. L. Auge, C. Laurent, D. Fabiani, and G. C. Montanari, "Investigating dc polyethylene threshold by space charge. Current and electroluminescence measurements," *IEEE Trans. Dielectr. Electr. Insul.*, vol. 7, no. 6, pp. 797–803, Dec. 2000.
- [141] L. A. Dissado, G. Mazzanti, and G. C. Montanari, "The role of trapped space charges in the electrical aging of insulating materials," *IEEE Trans. Dielectrics Electr. Insul.*, vol. 4, no. 5, pp. 496–506, Oct. 1997.
- [142] T. Mizutani, E. Nakane, K. Kaneko, and M. Ishioka, "Space charge dynamics in polypropylene," in *Proc. 17th Annu. Meeting IEEE Lasers Electro-Optics Soc. (LEOS)*, Oct. 2004, pp. 33–36.
- [143] B. Łowkis, "Parameters characterizing the charge state of dielectrics," *Mater. Sci.-Poland*, vol. 35, no. 3, pp. 601–605, Oct. 2017.
- [144] G. C. Montanari and D. Fabiani, "Searching for the factors which affect self-healing capacitor degradation under non-sinusoidal voltage," *IEEE Trans. Dielectrics Electr. Insul.*, vol. 6, no. 3, pp. 319–325, Jun. 1999.
- [145] J. Kurimsky, M. Kosterec, and B. Vargova, "Breakdown voltage of polypropylene film during C and thermal ageing," in *Proc. 18th Int. Sci. Conf. Electr. Power Eng. (EPE)*, May 2017, pp. 1–4.
- [146] M. Ieda, M. Nagao, and M. Hikita, "High-field conduction and breakdown in insulating polymers. Present situation and future prospects," *IEEE Trans. Dielectrics Electr. Insul.*, vol. 1, no. 5, pp. 934–945, Oct. 1994.
- [147] M. Ritamäki, I. Rytöluoto, and K. Lahti, "Temperature effect on breakdown performance of insulating polymer thin films," in *Proc. Nordic Insul. Symp.*, no. 24, Sep. 2017, pp. 75–79.
- [148] I. Rytöluoto and K. Lahti, "New approach to evaluate area-dependent breakdown characteristics of dielectric polymer films," *IEEE Trans. Dielectrics Electr. Insul.*, vol. 20, no. 3, pp. 937–946, Jun. 2013.



**HAIDER M. UMRAN** received the B.Sc. and M.Sc. degrees in electrical engineering from the University of Technology, Baghdad, Iraq, in 1998 and 2002, respectively. He is currently pursuing the Ph.D. degree with Chongqing University, China. He has been worked with the Ministry of the Industry and Menials, Iraqi. He became a Faculty Member of the Faculty of Engineering with Karbala University, in 2012. His research focuses on dielectrics and electrical insulation.



**FEIPENG WANG** (Member, IEEE) received the Ph.D. degree in materials physics and chemistry from Tongji University, China, in 2007. He was with the Applied Condensed-Matter Physics Group, University of Potsdam, and the Fraunhofer Institute for Applied Polymer Research, Germany, from 2007 to 2013, with a focus on functional dielectrics and their applications. Since 2014, he has been a Professor with Chongqing University, China, with an emphasis on engineering dielectrics and applications in power grids.



**YUSHUANG HE** received the B.Sc. degree in electrical engineering and automation from Northeast Petroleum University, Daqing, China, in 2017. She is currently pursuing the Ph.D. degree in electrical engineering with Chongqing University. Her major research field is dielectrics and electrical insulation.

• • •